geosciences

MDPI

Article

Dancing Towards the End—Ecological Oscillations in Mediterranean Coral Reefs Prior to the Messinian Salinity Crisis (Calcare di Rosignano Formation, Acquabona, Tuscany, Italy)

Giovanni Coletti [1], Alberto Vimercati [1], Francesca R. Bosellini [2], Alberto Collareta [3,*], Giulia Bosio [3], Adriano Guido [4], Alessandro Vescogni [2], Daniela Basso [1] and Or M. Bialik [5,6,7]

[1] Dipartimento di Scienze dell'Ambiente e della Terra, Università degli Studi di Milano-Bicocca, 20126 Milano, Italy; giovanni.coletti@unimib.it (G.C.); a.vimercati13@campus.unimib.it (A.V.); daniela.basso@unimib.it (D.B.)
[2] Dipartimento di Scienze Chimiche e Geologiche, Università di Modena e Reggio Emilia, 41125 Modena, Italy; francesca.bosellini@unimore.it (F.R.B.); alessandro.vescogni@unimore.it (A.V.)
[3] Dipartimento di Scienze della Terra, Università di Pisa, 56126 Pisa, Italy; giulia.bosio.giulia@gmail.com
[4] Department of Biology, Ecology and Earth Sciences, University of Calabria, 87036 Rende, Italy; adriano.guido@unical.it
[5] Institute of Geology and Paleontology, University of Münster, 48149 Münster, Germany; obialik@uni-muenster.de
[6] Dr. Moses Strauss Department of Marine Geosciences, The Leon H. Charney School of Marine Sciences, University of Haifa, Carmel 31905, Israel
[7] Israel Oceanographic and Limnological Research, National Institute of Oceanography, Haifa 310800, Israel
* Correspondence: alberto.collareta@unipi.it

Abstract: The lower Messinian Calcare di Rosignano Formation (Tuscany, Italy, 43° N) preserves one of the youngest and northernmost examples of coral reefs in the Mediterranean. The outcropping succession of the Acquabona quarry consists of four main facies, namely, in ascending stratigraphic order: (1) coral boundstone, (2) coralline algal rudstone, (3) serpulid floatstone to packstone, and (4) peloidal packstone to grainstone. The succession displays a trend toward increasingly more shallow conditions and progressively more restricted water circulation. The coral reef displays a limited coral biodiversity and a remarkable abundance of heterotrophs, similar to modern coral reefs developed at the edges of the ecological niche of symbiont-bearing colonial corals. The widespread presence of coral colonies pervasively encrusted by coralline algae and benthic foraminifera suggests that short-term environmental perturbations caused temporary shutdowns of the coral-dominated carbonate factory. Moving upwards, there are fewer corals and more highly adaptable carbonate producers like coralline algae and serpulids. This suggests that the decline of corals had been caused by the conditions in the basin becoming more stressful, up to the collapse of the coral community. The overall succession indicates that coral-dominated ecosystems located at the edges of the coral zone are very sensitive; they can be affected even by minor perturbations and easily collapse if negative conditions persist.

Keywords: *Porites*; encrusting foraminifera; coralline algae; serpulids; decapods; Miocene; shallow-water carbonates; Tora-Fine Basin

Citation: Coletti, G.; Vimercati, A.; Bosellini, F.R.; Collareta, A.; Bosio, G.; Guido, A.; Vescogni, A.; Basso, D.; Bialik, O.M. Dancing Towards the End—Ecological Oscillations in Mediterranean Coral Reefs Prior to the Messinian Salinity Crisis (Calcare di Rosignano Formation, Acquabona, Tuscany, Italy). *Geosciences* **2024**, *14*, 285. https://doi.org/10.3390/geosciences14110285

Academic Editor: José Manuel Castro

Received: 18 September 2024
Revised: 16 October 2024
Accepted: 23 October 2024
Published: 25 October 2024

1. Introduction

Symbiont-bearing colonial corals (i.e., colonial corals harboring in their living tissues unicellular photosynthetic dinoflagellates, the zooxanthellae, which live in a mutually beneficial symbiotic relationship with their host) are one of the primary shallow-water calcifiers of the late Cenozoic, inhabiting an environmentally narrow ecological niche in the photic zone of tropical seas [1,2]. This narrow niche is currently severely threatened by the ongoing climate change [3–6]. Warming and eutrophication result in the massive loss of coral domains with bleaching events becoming increasingly common [7–9].

At the edges of this niche, i.e., at higher latitudes, in restricted marginal marine environments and in turbid water settings, symbiont-bearing coral communities display the full extent of their ability to adapt [10–16]. It has been proposed that these somewhat 'extreme' settings can even serve as refugia against certain environmental fluctuations. For example, relatively high-latitude settings may prove favorable for low-latitude taxa under the current conditions of anthropogenic global warming [17–19].

However, living on the fringes has its disadvantages. Indeed, when the environmental conditions at a reef site exceed the ecological threshold suitable for corals, the coral community may quickly collapse. Recovery is not guaranteed even if optimal conditions are subsequently restored, and the aftermath of a coral reef demise is a debated topic [20–22]. Despite the growing body of literature on the recovery of modern coral reefs from bleaching events [23–27], these neontological case studies can only figure out what happens in the few years that follow the environmental perturbation. The study of the geological record is required to understand the long-term pattern of response and (potential) recovery of coral reef systems [12,28–30].

During the Messinian, Mediterranean coral reefs had to deal with multiple stressors, including enhanced glacioeustatic oscillations [31], temperature and nutrient variations [32–35], and a progressively more restricted basin [36]. The transition from the early Cenozoic greenhouse conditions to the near-modern icehouse conditions indeed occurred during the Miocene, with the Late Miocene atmospheric pCO_2 reaching values similar or only slightly higher than the current ones [37]. The tectonically driven restriction of the Mediterranean also added new layers of sensitivity to orbital forcing to the basin, notably with respect to salinity [38,39]. Yet, despite these multiple stresses, this period was associated with the development of common, widespread, euphotic coral reefs in the Mediterranean [33,34,40–42] (Figure 1), making the Late Miocene of the Mediterranean the ideal setting for investigating the response of coral reefs to environmental stressors.

The reef complexes of the Calcare di Rosignano Formation of Tuscany (central Italy), which developed during the Late Miocene, provide a relevant example of the behavior of coral reefs at the margins of their own ecospace. These bioconstructions were located at the northern edge of the reefs' distribution in the Mediterranean during the Messinian, with the Acquabona outcrop representing the northernmost, large-sized coral reef of the period [43,44]. Having developed at the periphery of the coral reef belt, the Acquabona reef represents a key example of the response and adaptability of corals to stressed marginal marine conditions. By integrating quantitative and qualitative analysis, the present paper analyzes short-term as well as long-term ecological succession in the Acquabona reef and interprets their paleoenvironmental relevance. Microfacies evidence can provide information on the aftermath of competition processes between reef-building organisms as well as snapshots on this long-lost ecosystem. In addition, the analysis of the succession can shed light on how this ecosystem evolved through time. Together, they disclose precious information that can more directly correlate with modern reefal environments, thus delivering useful insights to envision the future of coral reefs.

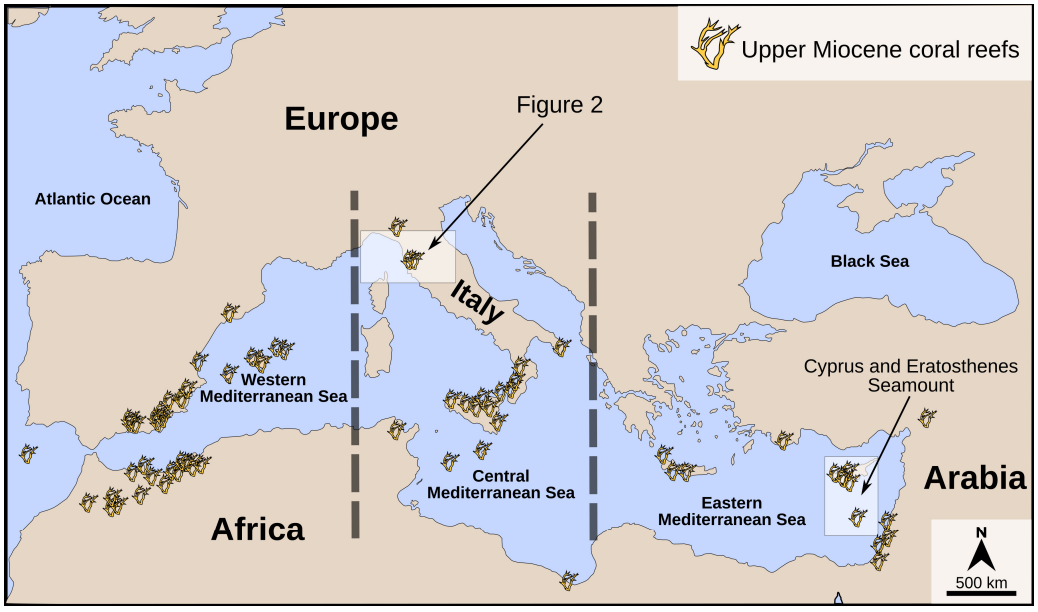

Figure 1. Distribution of the most relevant Upper Miocene coral reef outcrops of the Mediterranean area (after Perrin and Bosellini [33] and Franseen et al. [45]). The area depicted in the subsequent Figure 2, including the study site, is also indicated herein.

2. Paleogeography, Paleoclimate, and Coral Reefs in the Mediterranean During the Late Miocene

Modern equatorial currents predominantly move from East to West [46], leading the coral larvae to spread westward from the coral-rich Indo-West Pacific [47]. During the earliest Miocene, the (proto-)Mediterranean was connected to both the Atlantic and the Indo-Pacific Oceans [48], thus representing a wide and deep seaway for Indian Ocean-derived waters [49,50]. Climate models support a westward flow also during the Early Miocene [51], and the fossil record indicates that the Indo-Pacific has been a marine biodiversity hotspot for at least the last 25 million years [52]. Because of this, during the earliest Miocene, current-driven larval distribution patterns likely allowed for species to enter the Mediterranean basin from the tropical Indian regions, following the modern distribution pathways of larvae [53]. Such a connectivity was lost during the Burdigalian, as the connection with the Indo-Pacific narrowed and closed for the first time, only to reopen intermittently (as a shallow seaway) until the Langhian–Serravallian transition [48,50,54,55]. At about the same time, the connection with the Paratethys was also lost [56], although some intermittent exchange would temporarily occur until the Late Miocene [57]. At the beginning of the Late Miocene, the Central Mediterranean was still relatively well-connected with the Atlantic Ocean [58], whereas the Eastern Mediterranean had begun to experience restricted circulation. In spite of that, corals do not seem to show any clear endemism in the various Mediterranean sub-basins during the latest Miocene [34], although the diminishing connectivity should have led to higher degrees of endemicity [59,60].

During the Late Miocene, the global climate saw an overall cooling trend that started after the Middle Miocene Climatic Optimum (17 to 15 Ma) [61]. As early as in Tortonian times (11.61–7.25 Ma), the volume of the East Antarctic Ice Sheet was comparable to the present one [62], and the Arctic glaciations accelerated, resulting in an increase of the latitudinal and seasonal temperature gradients [63]. During the Messinian (7.25–5.33 Ma), cooling affected the mid- to high-latitude regions, thus bringing their sea surface temperatures to nearly modern values, whereas only a minor drop in temperature was recorded in the tropics [62].

This mid- to high-latitude cooling resulted in a decrease in the biodiversity of reef corals, reef fishes, and bryozoans across the Mediterranean region [64,65].

Paleoproductivity indicators (including organic matter accumulations and microfossil assemblages) in the Mediterranean suggest marine biogenic blooms during the Late Miocene—Early Pliocene interval [66], which are likely related to local increases of fluvial inputs [67] as well as to a global dust-driven fertilization of marine ecosystems [68]. Two major washhouse events are recognized in the Tortonian of the Mediterranean, at 10.7 Ma–9.7 Ma and around 8.9 Ma [35,69]. During these events, the average precipitations increased to ca. 200% above present-day values, which led to freshwaters entering the Mediterranean at an increased rate [35].

The Tortonian distribution of the symbiont-bearing colonial corals within the Mediterranean shifted southwards compared to the Serravallian. This shift is attributed not to changes in trophic or paleoceanographic conditions but rather to the progressive cooling of the global climate [33]. In spite of this cooling, Tortonian shallow water carbonates are rich in symbiont-bearing colonial corals. Notable and well-studied outcrops are located in southern Spain [70–74]; the Balearic Promontory [70,75,76]; northern Morocco, Algeria, and northern Italy (although no proper reefs have ever been reported in the latter area) [33,70,77]; southern Italy [70,78,79]; the Hyblean shelf [80–82]; Malta and Lampedusa [82–86]; Crete [87,88]; southern Turkey [89]; Cyprus [90,91]; the Eratosthenes Seamount [92,93]; and Libya [94] (Figure 1). Notably, the vast majority of these coral-bearing carbonates developed during the late Tortonian [33,42], after the aforementioned washhouse events [35].

During the Messinian, the progressively cooling climate reduced both the geographical distribution of symbiont-bearing colonial corals and their genus-level diversity within the basin [33,64,95]. Nonetheless, a large number of coral-bearing, shallow-water carbonates and reefs are known from the early Messinian of the Mediterranean, with notable outcrops occurring along the coasts of southeastern Spain [96–101]; Northern Morocco and Algeria [70,77,102]; northern Italy [70,103,104]; Tuscany [44]; Apulia [105–107]; Calabria, northeastern Sicily, Lampedusa, and Malta [82,84,108–113]; the Tell Mountains of Tunisia [114]; and Turkey, the Sirte Basin, and Israel [33,115] (Figure 1).

Towards the end of the Messinian, the tectonic activity in the Alboran Sea resulted in reducing the water exchanges between the Mediterranean Sea and the Atlantic Ocean, thus leading to the Messinian salinity crisis (MSC) (5.97 to 5.33 Ma) [116] and the basin-wide deposition of evaporites [117–119]. This unparalleled event led to a major crisis in Mediterranean ecosystems whose extent and magnitude has long been, and still is, debated [120–122].

3. Local Geological Setting

The Messinian Calcare di Rosignano Formation was deposited along the eastern margin of the Tyrrhenian oceanic basin, within what is currently known as the Tora–Fine Basin [123–125]. The latter is one of the many basins that developed parallel to the adjoining Northern Apennine mountain chain, being separated from each other by fringes of topographic highs, during a Neogene extensional tectonic phase (Figure 2).

The basement of the study area consists of the so-called Ligurian units, i.e., igneous and sedimentary rocks (mostly Jurassic radiolarites, serpentinites, basalts and gabbros, and Cretaceous deep-water sediments) pertaining to the Ligure-Piemontese oceanic basin [44]. This basement is overlain by upper Tortonian to lower Messinian lacustrine sediments (the Castello di Luppiano, Argille del Torrente Fosci, and Torrente Sellate formations, i.e., the so called “Serie Lignitifera”) and by the Calcare di Rosignano Formation [44,126]. The latter either overlies the lower Messinian lacustrine sediments or directly contacts the Ligurian basement [44]. It has been assigned to the lower Messinian based on its planktic foraminiferal assemblages [44].

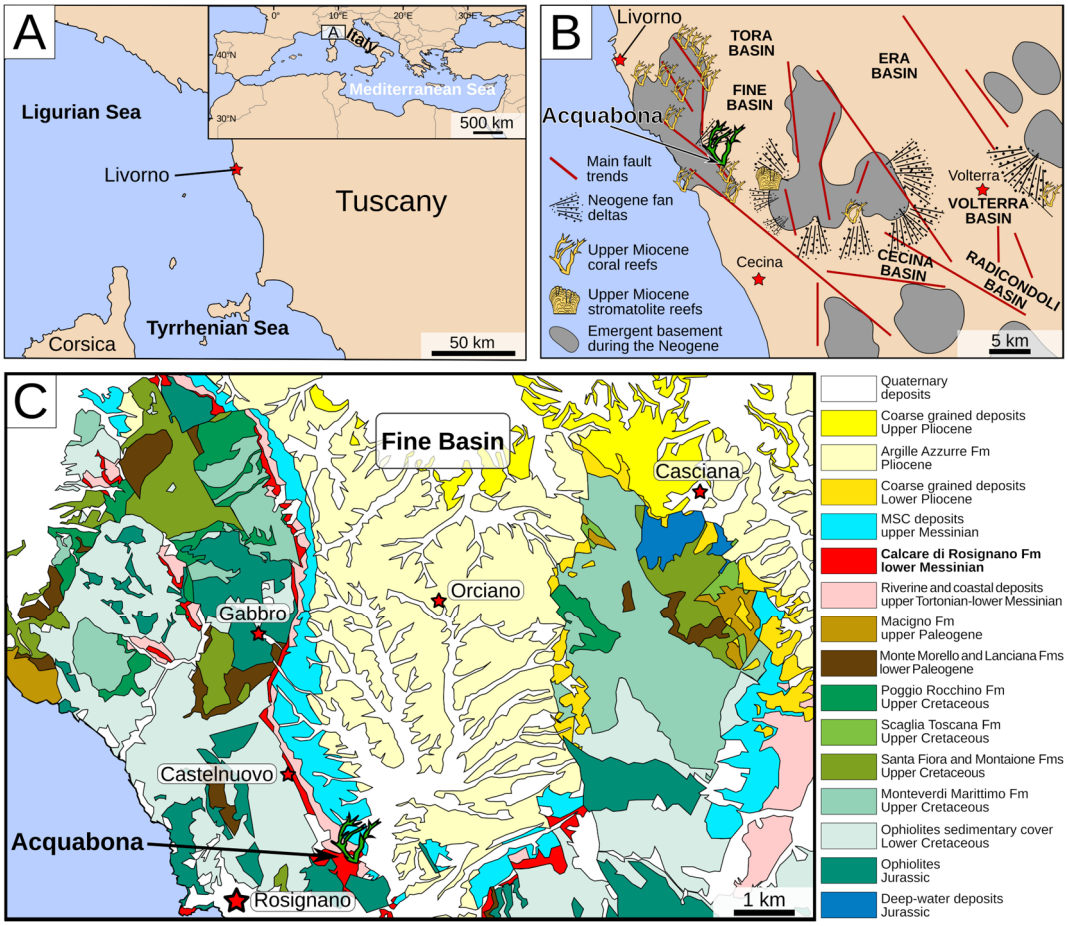

Figure 2. Study area. (**A**) Regional view of the study area with the position of the latter indicated in the Mediterranean Sea. (**B**) Schematic paleogeography of the Neogene and Quaternary basins between Livorno and Volterra, showing the locations of reef outcrops, including the investigated reef of the Acquabona quarry, coastal fans, fault trends, and emerging areas; modified from Bossio et al. [44]. (**C**) Simplified geological map of the study area; modified from Mazzanti et al. [126]. Fm = Formation; MSC = Messinian salinity crisis.

The Calcare di Rosignano Formation includes basal conglomerates (the informally named Cantine Conglomerates, rich in pebbles issued from the mafic basement of the basin); large coral-dominated bioconstructions and the related bioclastic carbonates; lagoonal bioclastic carbonates; small coral-dominated bioconstructions associated with coarse-grained siliciclastic deposits; and stromatolites [44,126,127]. These deposits have been informally divided into different bioclastic sub-units: the Acquabona reef, the lagoonal interval, and the Castelnuovo reef (ordered in ascending stratigraphic order). These bioclastic sub-units are separated from each other by subaerial exposure surfaces as well as by coastal terrigenous siliciclastic wedges with a minor bioclastic component (i.e., the Villa Mirabella and Sant'al Poggio conglomerates [44]). Different subdivisions have been proposed by other authors, and a formal separation of the formation is not currently available [128]. The Acquabona reef, representing the focus of this research, is located in a quarry complex. It is mainly composed of biogenic carbonates, while the Castelnuovo reef outcrops discontinuously, as small mounds, in various localities in the Livornesi Mountains and displays a relevant siliciclastic fraction [44].

4. Materials and Methods

The investigated succession of the Acquabona reef is located within an abandoned quarry that is currently used as an archery range (43°25′03.2″ N; 10°28′21.9″ E). It consists of

a sub-vertical quarry wall that is now partly covered by vegetation. Mesoscale observation of facies, distribution of macrofossils, and sample collection were carried out on the outcrop across multiple visits. The carbonate rocks were classified using the grain size categories of Wentworth's [129] scale as well as the Dunham's [130] classification as expanded by Embry and Klovan [131] and further refined by Lokier and Al Junaibi [132]. Given the intricacy of sampling within a massive boundstone displaying no clear bedding surfaces, large rock samples were collected from the core of the reefal structure outward, following the strike of the overlying layered strata. Twenty-four thin sections were prepared via repeated embeddings in epoxy resin in order to consolidate the poorly lithified and porous samples. Thin sections were then studied using a Leica Leitz Laborlux S transmitted light optical microscope and a Kenyans digital microscope to investigate the microfacies and textures. The skeletal assemblages were examined and quantified with point counting [133], using a 200 μm grid and counting more than 800 points in each section. This quantitative approach, combined with the updated carbonate rock classification developed by Lokier and Al Junaibi [132], provides a reasonably objective framework for describing the facies and fostering their comparison with coeval examples across the Mediterranean. In order to better constrain the foraminiferal assemblages of all sections, the free-living benthic foraminifera were identified at the lowest possible taxonomic level, divided between large symbiont-bearing forms (LBF) and small, non-symbiont bearing ones (SBF), and finally counted [134]. Furthermore, the community of secondary encrusters developing over the frame-building colonial corals was investigated in detail. Such a community was compared with those of the Upper Miocene reefs of Cyprus and Eratosthenes Seamount [91,92].

5. Results

The Acquabona reef outcrop consists of a nearly vertical rock wall cut through a hillside. At the core of the reef, the rock consists of ca. 10 m thick massive boundstone (Figure 3). Upwards, the boundstone is overlain by layered strata that gently dip northeastward. Moving along the dip direction, the massive boundstone progressively disappears underground, and the height of the rock wall progressively decreases. There is no indication other than dipping that the succession has been disturbed tectonically, which allows for a stratigraphically ordered sampling nearly perpendicular to the bedding direction indicated by the layered strata overlaying the bioconstruction.

Four main lithofacies can be recognized at the Acquabona outcrop: (1) coral boundstone, (2) coralline algal boundstone to rudstone, (3) serpulid floatstone to wackestone, and (4) peloidal packstone to grainstone (Table 1) (Figures 3–11).

The core of the bioconstruction is formed by a primary framework of coral (Figure 3). This boundstone facies consists mainly of large colonies of *Porites*, most of which display a branched columnar growth form (Figures 3D and 4A,B). The corals are poorly preserved, being either recrystallized or preserved as molds. Thick encrustations of coralline algae and encrusting foraminifera can be observed on the best-preserved coral specimens (Figure 4C). Small patches of sediment trapped among the colonies are also present, including well-preserved regular echinoids, disarticulated decapod appendages, and much rarer carapaces, bivalve shells (including pectinids and *Spondylus* sp.), and molds of gastropods (including Conidae, large-sized Vermetidae, and forms provided with turbinate and trochoid shells) (Figure 4D–F). Microfacies analyses of the coral boundstone reveals that the skeletal fraction (i.e., the bioconstructors and the hard-shelled organisms associated within the bioconstruction) accounts for between half and two-thirds of the rock volume (Figure 5A–C; Table 1). Frame builders (i.e., reef corals, coralline algae, and encrusting benthic foraminifera) represent >80% of the skeletal fraction (Table 1), and, as such, the vast majority of the rock volume of the reef, thus characterizing the latter as a frame reef [135]. The remaining volume consists of a very fine sand-sized to mud-sized matrix, with scattered fine sand-sized, angular, unidentified allochems (possibly originating from the fragmentation of the coral skeletons) (Figure 5D).

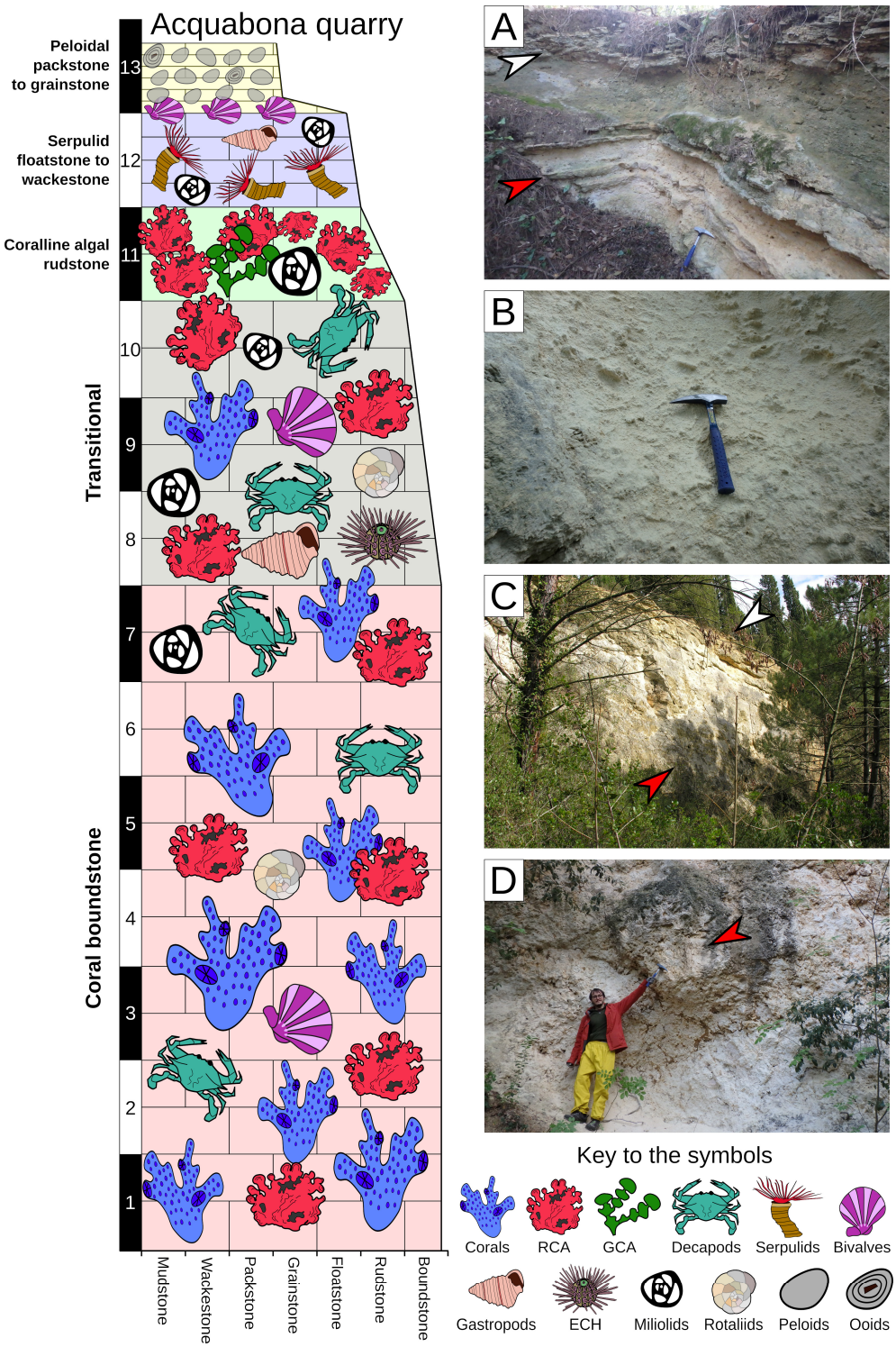

Figure 3. The investigated succession of the Acquabona quarry, with a stratigraphic log (meters from the base of the section are indicated in the black-and-white bar on the left). (**A**) Serpulid floatstone to wackestone (red arrowhead) and peloidal packstone to grainstone (white arrowhead). (**B**) Transition from the coral boundstone (periphery) to the coralline algal rudstone. (**C**) Landscape view of the outcrop, taken in 2007, showing the massive coral boundstone (red arrowhead) overlain by the gently dipping layered strata of the upper part of the succession (white arrowhead). The red arrowhead is substantially in the same position as in panel D, and the whole rock face is ca. 10 m high. (**D**) Coral boundstone facies with a large branched *Porites* colony (red arrowhead). RCA = Red calcareous algae; GCA = green calcareous algae; ECH = echinoderms.

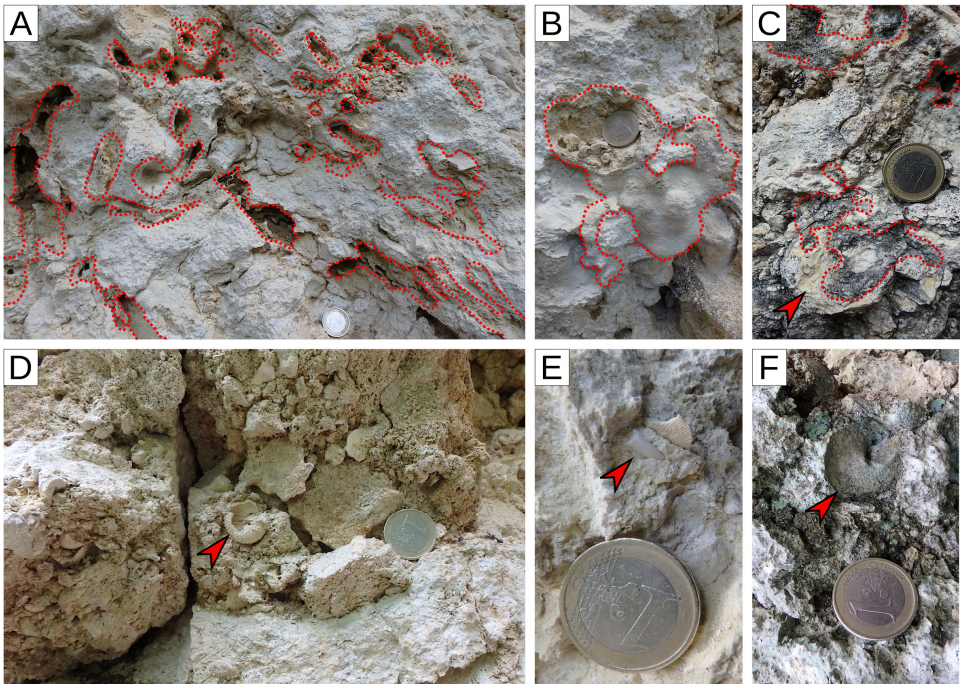

Figure 4. Macrofossils of the coral boundstone lithofacies. (**A**) Partially dissolved columnar colonies of the genus *Porites* (outlined by red dashed lines). (**B**) A moderately well preserved colony of *Porites* (outlined by red dashed lines). (**C**) Coral colonies (outlined by red dashed lines) encrusted by coralline red algae (red arrowhead). (**D**) Pocket of bioclastic sediment trapped within the bioconstructions and displaying a moderately well preserved test of sea urchin, possibly genus *Paracentrotus* (red arrowhead). (**E**) Decapod appendage (red arrowhead). (**F**) The internal mold of a Conidae (red arrowhead).

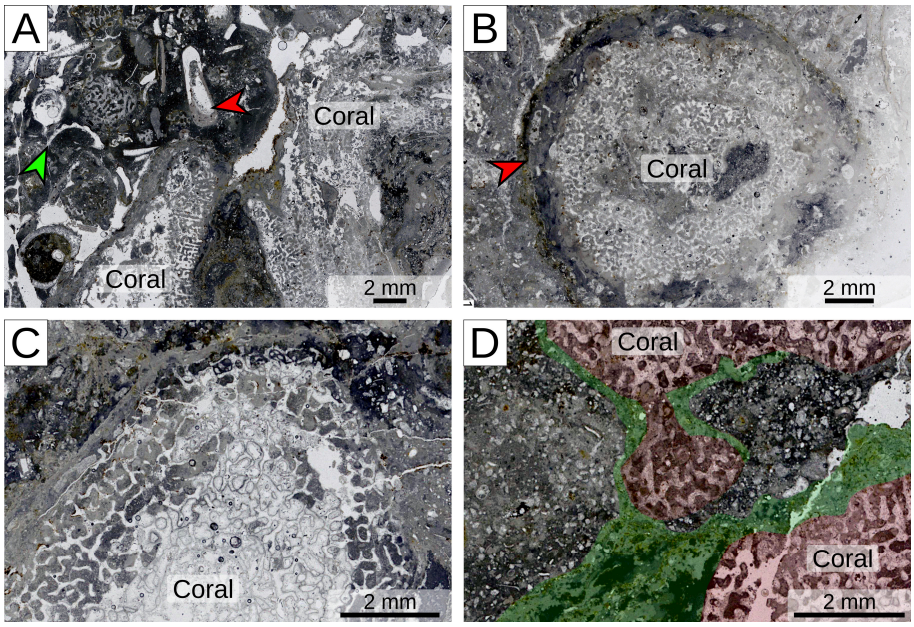

Figure 5. Microfacies of the coral boundstone lithofacies (corals). (**A**) Low magnification microphotograph of the coral boundstone, displaying abundant colonial corals but also large-sized fragments of decapod crustaceans (red arrowhead) and mollusks (green arrowhead). (**B**) Detail of an axial section of a branched coral colony completely encrusted by sclerobionts (red arrowhead). (**C**) Detail of the inner structure of a recrystallized coral colony. (**D**) Fine sand-sized angular grains and micrite trapped between sclerobiont-encrusted coral colonies. The red hue indicates the corals; the green hue indicates the sclerobionts (mainly nubeculariids and coralline algae).

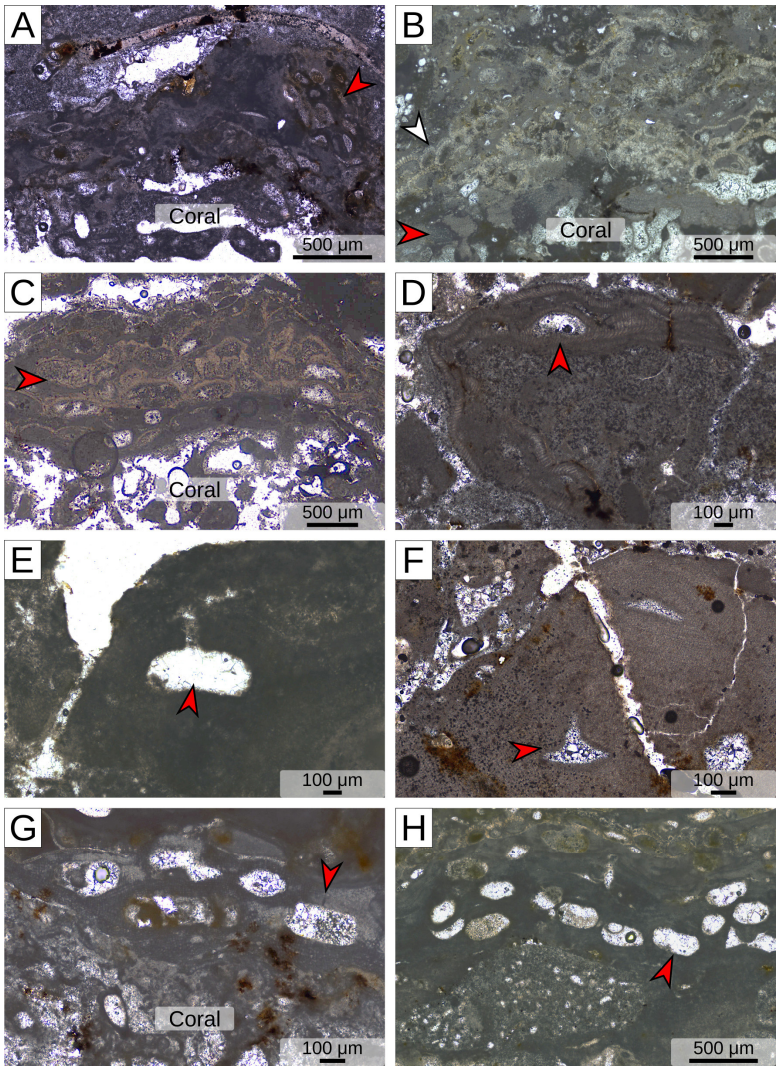

Figure 6. Microfacies of the coral boundstone lithofacies (encrusting organisms). (**A**) Encrusting porcelaneous foraminifera (nubeculariids; red arrowhead). (**B**) Encrusting coralline algae (red arrowhead) and encrusting hyaline foraminifera (*Homotrema* sp.; white arrowhead). (**C**) Encrusting bryozoans (red arrowhead). (**D**) Encrusting coralline alga of the genus *Titanoderma*, order Corallinales; red arrowhead = uniporate conceptacle. (**E**) Fragment of a coralline alga tentatively attributed to the order Corallinales; red arrowhead = uniporate conceptacle. (**F**) Male gamentangial thallus tentatively ascribed to the order Corallinales; red arrowhead = uniporate conceptacle. (**G**,**H**) Sporangial thalli tentatively ascribed to the order Hapalidiales; red arrowhead = multiporate conceptacle.

Table 1. Skeletal assemblages, sedimentological, and petrographic characteristics of the facies of the Acquabona quarry outcrop investigated with point counting and foraminiferal area counting.

Lithofacies	**Coral Boundstone (Core)**	**Transition from the Coral Boundstone to the Coralline Algal Rudstone**	**Coralline Algal Rudstone**	**Serpulid Floatstone to Wackestone**
Thickness (m)	7	3	1	1
Skeletal fraction	1/2–2/3	1/3–1/2	1/2–2/3	1/4–1/3
Matrix	1/3–1/2	1/2–2/3	1/3–1/2	2/3–3/4
Composition of the skeletal assemblage (% point counting)				
Symbiont-bearing colonial corals	46	7.5	3	0
Red calcareous algae	26.5	39	66.5	0.5

Table 1. *Cont.*

Lithofacies	Coral Boundstone (Core)	Transition from the Coral Boundstone to the Coralline Algal Rudstone	Coralline Algal Rudstone	Serpulid Floatstone to Wackestone
Green calcareous algae	0.5	3.5	8.5	0
LBF	0	1	0	0
Encrusting benthic foraminifera	8.5	3	2	0
SBF	2	3	8	6.5
Planktic foraminifera	0	0	0	0
Mollusks	3	9.5	2	11.5
Echinoderms	4	9.5	2.5	19
Bryozoans	1.5	5.5	1.5	0
Serpulids	0	2	3	60.5
Ostracods	0.5	0.5	1	1.5
Decapods	7.5	16	2	0.5
Foraminiferal assemblage (area counting; individuals cm^2)				
Porcellaneous SBF	1.12	1.71	9.39	7.25
Hyaline SBF	2.04	2.13	10.34	8.46
Agglutinated SBF	0.03	0.02	0	0
Porcellaneous/hyaline ratio	0.55	0.75	0.91	0.86
P/B ratio	Entirely benthic	Entirely benthic	Entirely benthic	Entirely benthic

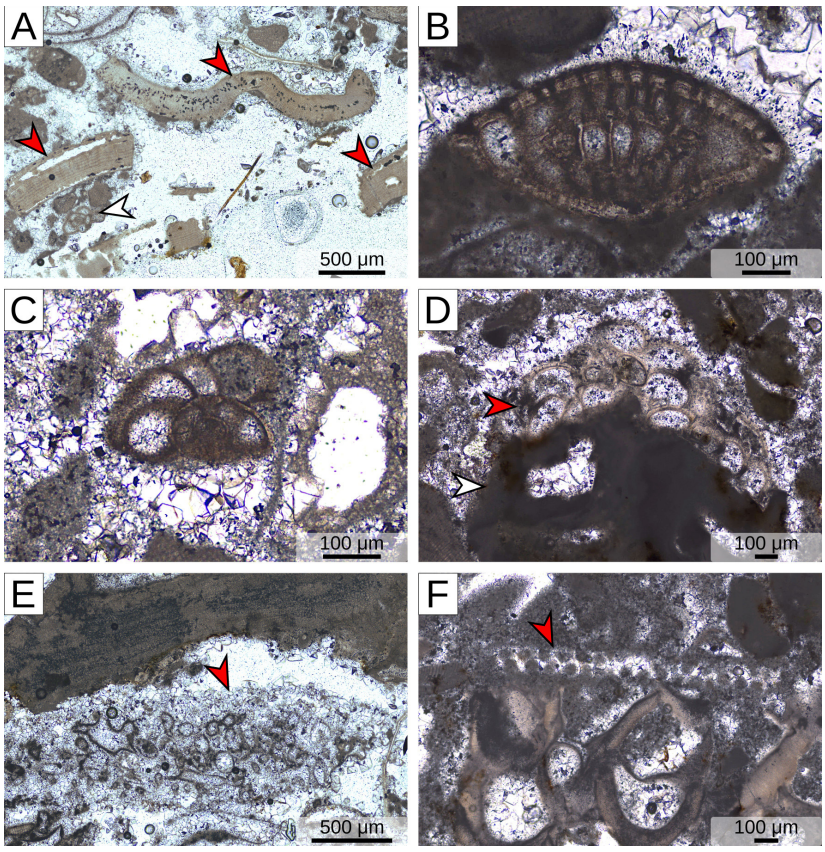

Figure 7. Microfacies of the coral boundstone lithofacies (decapods, benthic foraminifera, and green calcareous algae). (**A**) Fragments of decapods exoskeleton (red arrowhead). (**B**) *Elphidium* sp. (**C**) *Cibicides* sp. (**D**) *Planorbulina* sp. (red arrowhead) attached to a fragment of a crust consisting of nubeculariids (white arrowhead). (**E**) *Halimeda* sp. (red arrowhead). (**F**) *Acetabularia* sp. (red arrowhead).

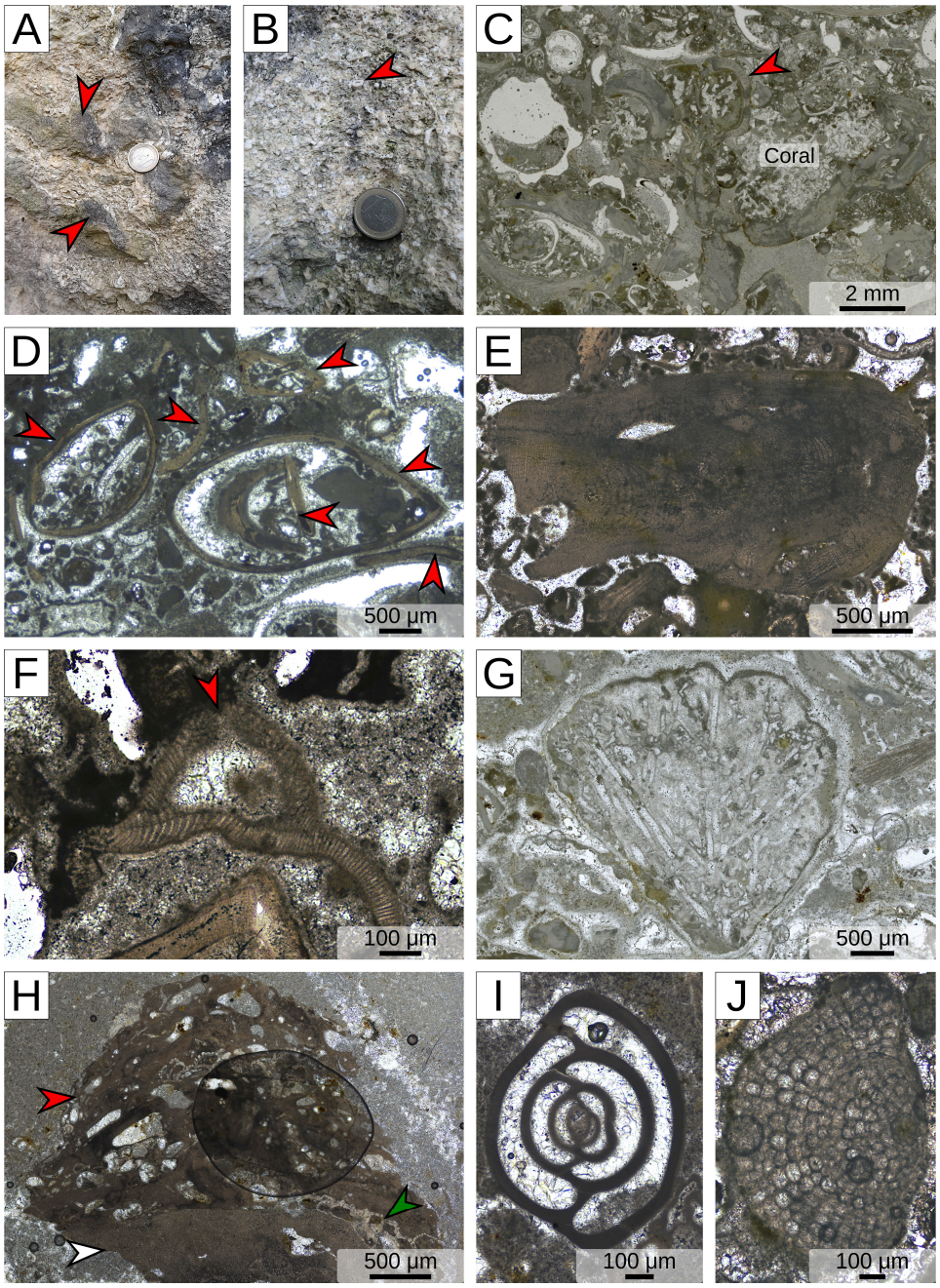

Figure 8. Transition between the coral boundstone lithofacies and the coralline algal rudstone lithofacies. (**A**) Scattered columnar colonies of *Porites* (red arrowhead). (**B**) Coarse-grained sediment trapped between coral colonies; decapod appendage = red arrowhead. (**C**) Low magnification image of the microfacies showing the primary skeletal framework of the boundstone composed of coralline algae and corals; red arrowhead = decapod fragment. (**D**) Decapod fragments (red arrowheads). (**E**) Thallus tentatively attributed to *Lithophyllum* cf. *dentatum* (order Corallinales). (**F**) Thin crust of the order Corallinales; red arrowhead = uniporate conceptacle. (**G**) Plate of *Halimeda* sp. (**H**) Multi-taxon encrustation, white arrowhead = coralline alga; red arrowhead = nubeculariid; green arrowhead = homotrematid. (**I**) *Pyrgo* sp. (**J**) *Discogypsina* sp.

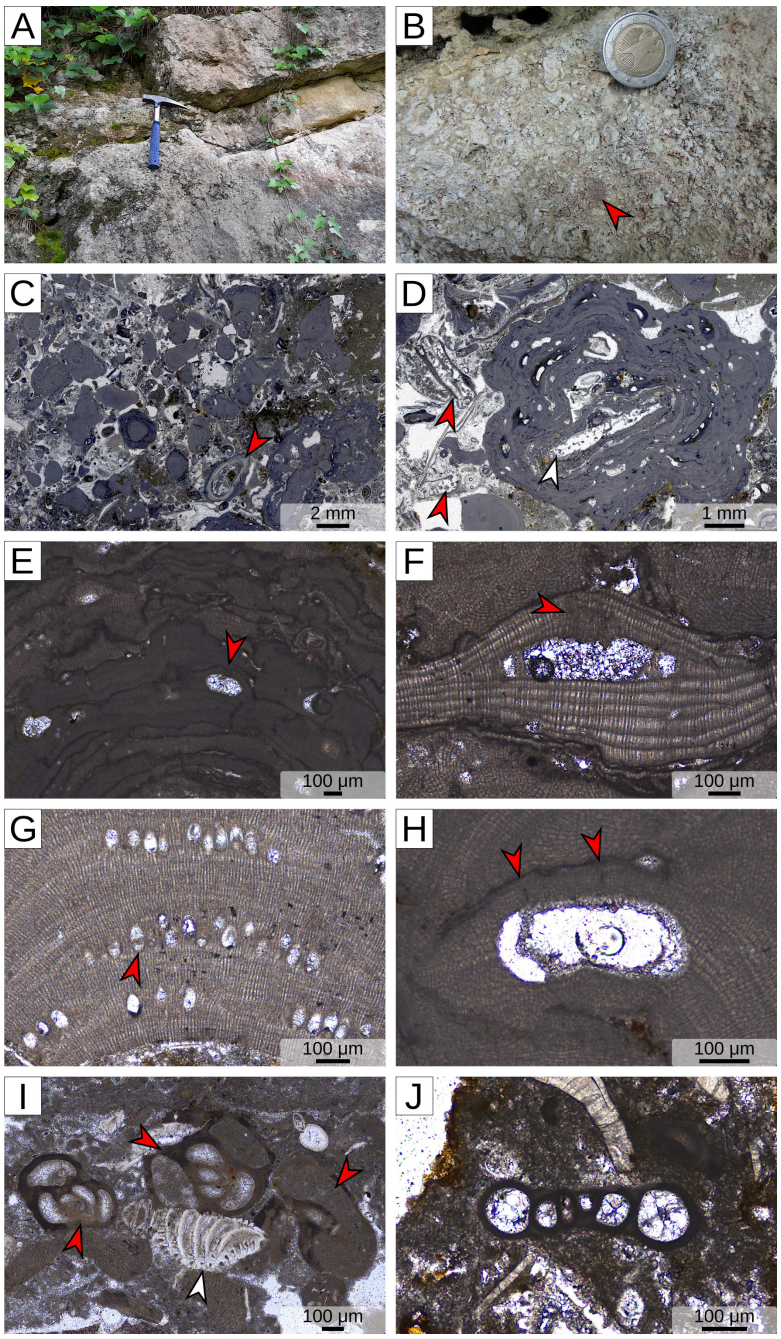

Figure 9. Coralline algal rudstone lithofacies. (**A**) Northeastward dipping strata characterized by the coralline algal-dominated facies. (**B**) Detail of the small and compact coralline algal nodules; red arrowhead = bryozoans. (**C**) Low magnification image of the microfacies; red arrowhead = serpulid. (**D**) Detail of a small compact coralline algal nodule growing over a fragment of *Halimeda* sp. (white arrowhead); other *Halimeda* sp. fragments are also present (red arrowheads). (**E**) Stacked coralline algal thalli constituting a nodule; red arrowhead = uniporate conceptacle (suggesting a placement within the order Corallinales). (**F**) *Titanoderma* sp. The red arrowhead indicates the stretching of the cells in the roof of the conceptacle in proximity of the pore canal, since the conceptacle is not properly cut, i.e., with a section crosscutting the pore canal, the canal cannot be seen properly; however, the stretching of the roof cells clearly highlights its presence. (**G**) *Sporolithon* sp.; red arrowheads indicates a stalk cell in a sporangial cavity. (**H**) Thallus tentatively attributed to the order Hapalidiales based on the presence of multiporate conceptacles (red arrowheads = pore canals). (**I**) Porcellaneus SBF (red arrowheads) and *Elphidium* sp. (white arrowhead). (**J**) *Spiroloculina* sp.

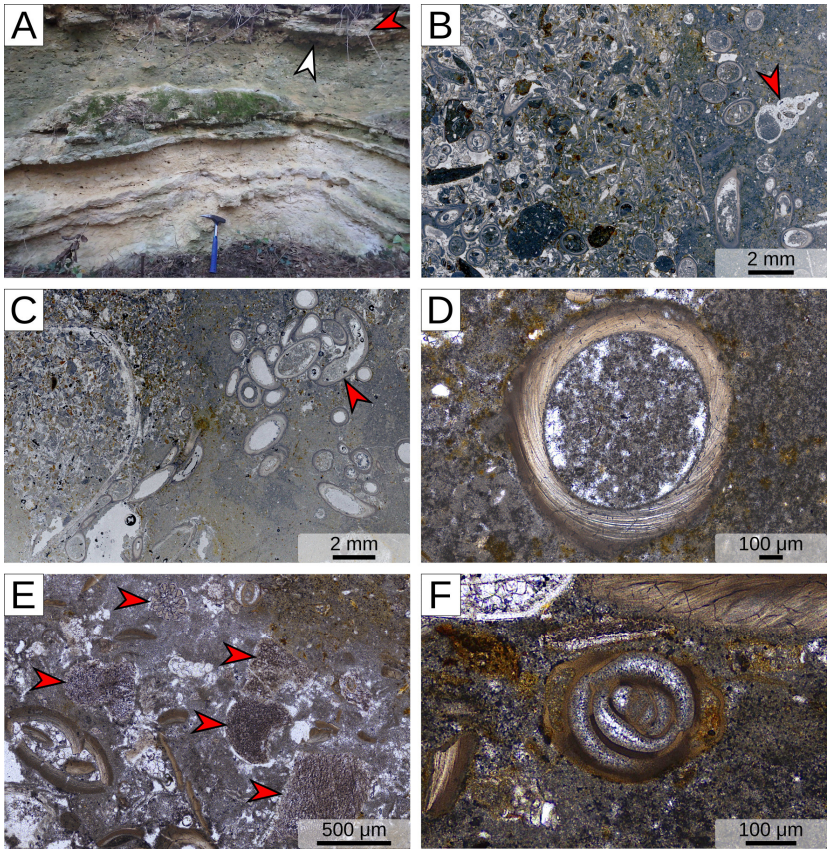

Figure 10. Serpulid floatstone to packstone lithofacies. (**A**) Northeastward dipping strata dominated by serpulids. Red arrowhead = the overlying peloid dominated facies; white arrowhead = layer with abundant articulated bivalve shells characterizing the base of the peloid dominated facies. (**B**) Low magnification image of the microfacies; red arrowhead = gastropod mold. (**C**) Low magnification image of the microfacies with cluster of serpulids (red arrowhead). (**D**) Detail of a serpulid. (**E**) Abundant echinoderm fragments (red arrowheads). (**F**) Porcellaneous SBF.

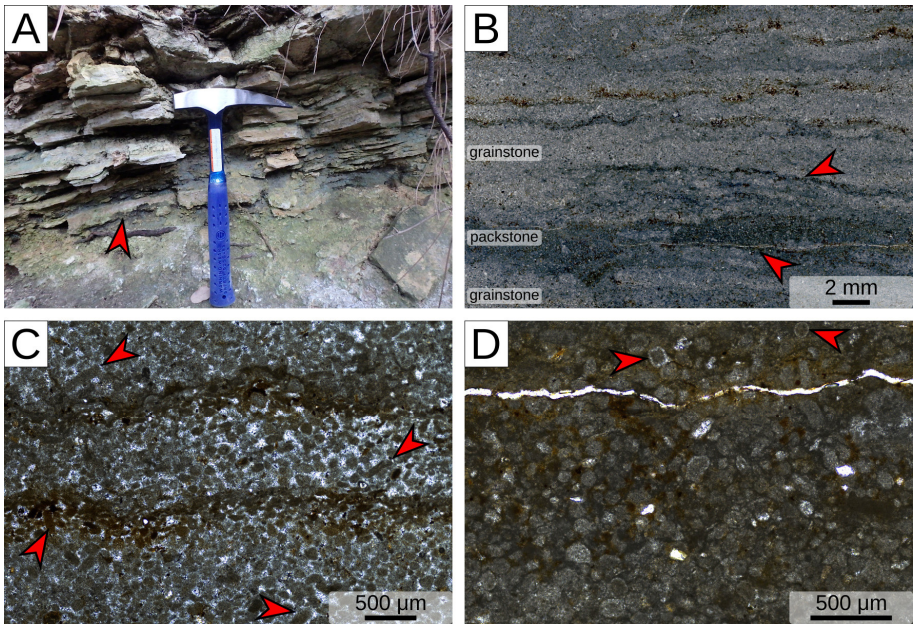

Figure 11. Peloid packstone to grainstone lithofacies. (**A**) Field photo of the fine-stratified peloidal lithofacies. (**B**) Overview of the peloidal microfacies showing the well-packed grain texture. Note

the alternation between the lighter grainstone laminae and grayish packstone laminae separated by erosive, frequently oxidized, boundaries (red arrowheads). (**C**) Detail of the grainstone laminae. Note the well-defined edges of the peloids and the cylindrical shape of some of them (red arrowheads), interpreted as fecal pellets. (**D**) Detail of the packstone laminae with a very dense peloidal texture. Note the rounded grains displaying cortical envelopments and thus representing possible ooids (red arrowheads).

The skeletal assemblage is dominated by colonies of the genus *Porites* (46% of the skeletal assemblage; between 1/4 and 1/3 of the whole rock) associated with coralline algae, encrusting benthic foraminifera, decapod crustaceans, echinoderms, mollusks, small free-living benthic foraminifera, bryozoans, green calcareous algae, and ostracods (in order of decreasing abundance) (Table 1; Figures 5–7). *Porites* colonies are almost invariably encrusted by a succession of sclerobionts (Figure 5B–D). The first generation of encrusters growing directly over the coral is usually represented by nubeculariids (encrusting porcellaneous foraminifera) and, more rarely, by coralline algae (Figure 6A–C,G). This initial generation of sclerobionts is commonly followed by a second layer of encrusting organisms, and often by a third. These later generations generally consist of coralline algae, encrusting porcellaneous foraminifera (nubeculariids), encrusting hyaline foraminifera (mainly homotrematids), or, more rarely, bryozoans (Figure 6A–C). Coralline algae are usually very poorly preserved or sterile (i.e., lacking reproductive cavities), making their taxonomic identification often impossible. Among the few specimens displaying diagnostic characters, some have been tentatively assigned to the order Corallinales (including the genera *Lithophyllum* and *Titanoderma*) (Figure 6D–F) and very few to the order Hapalidiales (Figure 6G,H). The foraminiferal assemblage is dominated by hyaline SBF, such as *Elphidium* spp., *Cibicides* spp., and rare *Planorbulina* sp., associated with relevant amounts of porcellaneous SBF, such as *Pyrgo* spp. (Table 1; Figure 7B–D). Green calcareous algae are very rare, but both *Halimeda* sp. and *Acetabularia* sp. can be recognized (Figure 7E,F).

Toward the periphery of the bioconstruction, the coral density decreases, whereas the amount and grain size of the sediment trapped between the colonies increases (Figures 3 and 8A,B). With the increase in grain size, the amount of micrite pore fill decreases, and cement becomes more common. The skeletal assemblage in this transition zone, between the bioconstructions and the overlying layered bioclastic sediments, is dominated by coralline algae (39% of the skeletal assemblage; between 1/6 and 1/5 of the whole rock) associated with decapod crustaceans, colonial corals, mollusks, echinoderms, bryozoans, encrusting foraminifera (both nubeculariids and homotrematids), free-living benthic foraminifera, green calcareous algae, and encrusting serpulids (Figure 8) (Table 1). Coralline algal preservation and the lack of fertile specimens prevent accurate taxonomic identification. The few specimens displaying elements useful for their identification have been assigned to the order Corallinales (Figure 8E,F). The green algae are mostly represented by *Halimeda* sp., but *Acetabularia* sp. also occur (Figure 8G). *Porites* colonies, as well as other large bioclasts, are still characterized by abundant encrustations of benthic foraminifera (both nubeculariids and homotrematids) and coralline algae (Figure 8H). Rare bryozoan encrustations also occur. The foraminiferal assemblage is dominated by hyaline SBF (including the genera *Elphidium* and *Cibicides*) associated with relevant amounts of porcellaneous SBF (including the genus *Pyrgo*) (Figure 8I). Rare specimens of the hyaline LBF *Discogypsina* sp. were also observed (Figure 8J). Although the composition of the foraminiferal assemblage is almost the same as in the core of the reef, an overall increase in the abundance of specimens (i.e., number of individuals in each mm^2 of the section) can be observed (Table 1).

The coral boundstone is overlain by a 0.5 m thick layer of well-sorted coralline algal rudstone with a packstone to grainstone matrix (Figures 3 and 8). It displays a dip of about 10–15° toward NE. The layer consists of an assemblage of small, compact rhodoliths (1–2 cm in diameter) and coralline algal branches (few centimeters in length and nearly one centimeter in thickness), associated with bryozoan colonies and aggregates of encrusting serpulids (Figure 9A,B). Upward, coralline algae are still dominant, but the abundance of mollusks (mostly oysters) and detrital micrite increases.

Based on the microfacies analysis, the skeletal material represents between half and two-thirds of the rock volume; the remaining part consists mainly of fine sand-sized, unrecognizable bioclastic grains and micrite (Table 1). The skeletal assemblage is largely dominated by coralline algae (66% of the skeletal assemblage; between 1/3 and almost 1/2 of the whole rock), associated with *Halimeda* sp., SBF, fragments of *Porites*, echinoderms, mollusks, serpulids, encrusting benthic foraminifera, bryozoans, decapod crustaceans, and very rare LBF (Table 1) (Figure 9). The coralline algal nodules generally display a compact structure (Figure 9C,D) and an assemblage dominated by Corallinales (including the genus *Titanoderma*) (Figure 9E,F) associated with Sporolithales and minor amounts of Hapalidiales (Figure 9G,H). The foraminiferal assemblage is dominated by porcellaneous SBF (including *Pyrgo* spp. and *Spiroloculina* sp.), associated with relevant amounts of hyaline SBF (including *Elphidium* spp., *Cibicides* spp., and *Planorbulina* sp.) and rare agglutinated SBF (Figure 9I,J). Rare specimens of *Discogypsina* sp. also occur. Overall, free-living benthic foraminifera are much more numerous than in the previous facies.

The coralline algal-dominated lithofacies is overlain by a serpulid floatstone to wackestone lithofacies (Figure 3). The latter consists of thin layers of well-lithified bioclastic limestone rich in serpulids (including small aggregates) and layers of poorly lithified marly limestone with lesser amounts of bioclasts (Figure 10A). They display an orientation similar to those of the underlying coralline algal-dominated layers. Overall, skeletal grains account for a quarter of the whole rock, and the remaining part consists of micritic matrix and very fine sand-sized unrecognizable bioclastic grains (Table 1).

The skeletal assemblage is largely dominated by encrusting serpulids (60% of the skeletal assemblage; between 1/7 and 1/5 of the whole rock) represented by clusters consisting of various specimens and by poorly sorted fragments (Figure 10B–E). Serpulids are associated with echinoderms fragments, mollusks (represented by molds of both bivalves and gastropods), small benthic foraminifera, ostracods, and decapod crustaceans (Table 1; Figure 10). The foraminiferal assemblage is dominated by porcellaneous and hyaline SBF (including the genera *Elphidium* and *Cibicides*) (Figure 10F). The abundance of fine-grained bioclasts and the absence of relevant microbialite textures, notably wrinkled lamination and/or clotted peloidal fabrics, account for a detrital origin of the micrites (allochthonous or detrital micrite).

The serpulid-dominated layers are overlain by ~0.5 m of well-lithified, laminated, peloidal packstone to grainstone facies (Figures 3 and 11A) whose base is characterized by a 2 cm thick horizon with small, articulated bivalve shells. Peloids are well-sorted and show a rounded to cylindrical shape and a size ranging from 100 µm to 200 µm (Figure 11B–D). The packed texture and the well-defined edges suggest that the peloids derive from the erosion and transport of micritized skeletons and cemented allochthonous micrite, like those observed in the other facies. A possible fecal origin of some of the pellets is suggested by the presence of cylindrical, sometime curved shape, of part of the peloids (Figure 11C). Micritic intraclasts are also present. These grains confirm the detrital origin of this facies. The alteration of the carbonates prevents detailed observation of the micro-texture, but some rounded grains display cortical envelopments, suggesting the possible presence of oolites (Figure 11D). Peloids are organized in regular, sub-parallel laminae characterized by different abundances of micrite (Figure 11B,C). The transitions between the two types of laminae (packstone vs. grainstone) often appear irregular, erosive, and rich in iron oxides (Figure 11B).

6. Discussion

6.1. Paleoenvironmental Interpretation

The primary framework of the bioconstruction is exclusively constituted by coral colonies belonging to the genus *Porites*. No other corals have been identified, thus confirming the low diversity and the dominance of the cosmopolitan and highly tolerant genus *Porites*, which characterizes all the Mediterranean Messinian reefs. The low diversity of the coral assemblage has been related to the gradual northwards shift of the Mediterranean

region outside the tropical belt and the closure of the seaway with the Indo-Pacific, together with the global cooling of sea surface temperatures [33,34,64,136].

The skeletal assemblage of the coral boundstone is dominated by photoautotrophs (e.g., calcareous algae) and mixotrophs (symbiont-bearing colonial corals). Together, they represent nearly 75% of the identified skeletal assemblage. Heterotrophs instead account for about 25% of the skeletal assemblage (including 10% from encrusting benthic foraminifera). In modern warm-water tropical settings, where light is the most available form of energy, skeletal assemblages are usually dominated by a mixture of photoautotrophs and mixotrophs [2]. Consistently, the skeletal assemblage of the investigated succession of the Acquabona reef is compatible with a light-dominated setting. Within this context, and notwithstanding its poor preservation, the coralline algal assemblage can provide further paleobathymetric information. The clear dominance of Corallinales over Hapalidiales suggests that the investigated reef should have developed at a water depth of 20 m or less [93,137]. A coralline algal assemblage dominated by Corallinales was also reported by Fravega et al. [127] in the small coral boundstone of the Castelnuovo reef (one of the other informal unit of the of the Calcare di Rosignano Formation) outcropping near Cafaggio (43°26′57.4″ N 10°26′49.9″ E), a few kilometers northward from the Acquabona outcrop. Based on this algal assemblage, Fravega et al. [127] postulated that the examined coral bioconstruction developed in the euphotic zone (sensu Pomar [138]). A shallow water context for the investigated coral boundstone is also indicated by the abundance of small porcellaneous foraminifera [139]. As the coral growth forms, the Acquabona reef does not show the typical zonation of several Messinian reefs [40,75,107], as it is mostly composed of branching columnar colonies. This coral shape has been described for the upper slope facies but also for very shallow reef tracts, and it has been explained as a fast growth response to relatively rapid sea-level changes or to increasing cooler and higher nutrient levels, or as a morphological adaptation to withstand high levels of fine-grained clastic sedimentation. Some good examples are represented by "thicket zones" (estimated to have developed at a water depth of up to 10 m) in the fringing reefs of Almeria Province of Spain [96,140], Algeria [112,141], some reefs of central Sicily (Caltanisetta Basin) and of the Pelagian Islands [82,110], and Apulia [106,107].

The shift from the coral boundstone to the coralline algal rudstone and then to the serpulid floatstone to wackestone can be interpreted as representing a shallowing of the depositional environment, and, as such, a regressive trend. Similar to the coral boundstone facies, the coralline algal rudstone is characterized by a clear dominance of Corallinales over Hapalidiales. Furthermore, the coralline algal rudstone displays small compact rhodoliths suggestive of considerable hydrodynamic energy [142]. Compared to the coral boundstone, the foraminiferal assemblage of the coralline algal rudstone displays a higher porcellaneous/hyaline foraminiferal ratio, such an increased abundance of porcellaneous foraminifera being suggestive of shallower water depths [134]. These elements suggest that the coralline algal rudstone might have developed landward from the reef, probably in a very shallow environment (possibly at less than 10 m of water depth). Large accumulations of serpulids are common in shallow lagoonal settings [143–146], suggesting that the serpulid floatstone to wackestone might represent an even shallower setting. This is also supported by the persistently high porcellaneous/hyaline foraminiferal ratio [134]. The increase in the mud fraction might instead be related to a decrease in hydrodynamic energy, possibly suggesting a marginal setting protected from the open sea by shoals. That said, no back reef facies was found in between, suggesting that this shift should represent an environmental change rather than a lateral transition.

The shallowing upward trend is further confirmed by the peloidal packstone to grainstone facies. The absence of bioclasts, together with the presence of intraclasts and small oolites, suggests a deposition of this facies in an intertidal setting characterized by a low hydrodynamic energy.

6.2. The Significance of the Acquabona Reef

To emphasize the general significance of the Acquabona outcrop in the framework of Upper Miocene shallow-water carbonate systems of the Mediterranean Basin, the skeletal assemblage of the coral boundstone have been compared to those of other Upper Miocene, coral-dominated, bioconstructions developed at lower paleolatitudes in the Eastern Mediterranean, namely Cyprus and the Eratosthenes Seamount (Figure 1).

The (heterotroph) vs. (mixotroph plus photoautotrophs) ratio in the Acquabona coral boundstone is essentially comparable to that of the Upper Miocene coral boundstone of Cyprus [91], but it is significantly higher than that of the Upper Miocene coral boundstone of the Eratosthenes that developed on an isolated seamount [92] (Table 2). At high latitudes, the amount of solar energy (photosynthetically available radiation) is reduced to levels that make the phototrophs less efficient and allow for a greater abundance of heterotroph carbonate producers [2]. Similarly, close to landmasses, where the supply of nutrients from river runoff is higher, heterotrophs are favored given the increased availability of food. Unlike photoautotrophs and mixotrophs, heterotrophs rely only on the chemical breakdown of food particles for living, and, as such, they thrive wherever solar energy is not the dominant form of available energy [2]. Therefore, the higher abundance of heterotrophs in the Acquabona reef compared to the Eratosthenes reef is consistent with one being located close to a landmass and the other on an isolated seamount (Figure 1). Although this is already a relevant element, it is noteworthy to mention that in all the three examples of Upper Miocene coral reefs, a sizable share of heterotroph carbonate producers is represented by encrusting benthic foraminifera, a group whose life strategy is still poorly understood [147–150]. Indeed, while certain living taxa of encrusting benthic foraminifera may harbor photosymbionts (e.g., *Gypsina plana* [151,152]; *Homotrema rubrum* [153]), others do not [154]. Understanding whether or not a fossil encrusting benthic foraminifera hosted photosymbionts is obviously more complex. This leads to even greater uncertainties regarding to their environmental significance with respect to the heterotrophs vs. (mixotroph + photoautotrophs) ratio. Studies on the modern distribution of *Nubecularia* and *Homotrema* (which are the closest living relatives of the two most common types of encrusting benthic foraminifera in the analyzed Upper Miocene deposits) show that, at tropical latitudes, both genera (especially *Nubecularia*) clearly favor well-lit, shallow-water settings [152,155]. It is thus reasonable to infer that their distribution is somewhat limited or controlled by light. Since nubeculariids and homotrematids represent the majority of the encrusting benthic foraminifera recognized in the Upper Miocene coral boundstones of Acquabona, Cyprus, and Eratosthenes [91,92], analyzing the percentage of heterotrophs, excluding encrusting benthic foraminifera, may provide further useful information. By doing so, the results indicate that the Acquabona boundstone displays a significantly higher percentage of heterotrophs compared to the other two sites, consistent with its northerly position and its proximity to landmasses compared to the other two sites (Table 2), further showcasing the similarity between the Late Miocene Mediterranean carbonate systems and modern carbonate systems.

Among heterotrophs, decapod crustaceans (shrimps, crabs and kin) are particularly relevant in the investigated Acquabona succession. They represent more than 5% of the skeletal assemblage in the coral boundstone, and nearly 15% of the assemblage at the transition between the coral boundstone and the coralline algal rudstone [Table 1]. In both cases, they are the most common type of free-living carbonate producers in the assemblage. This comes as no surprise, as crabs represent one of the most diverse components of the present-day coral reefs communities [156], and *Porites*-dominated bioconstructions are no exception, as reported by Abele [157] for the living *Porites* colonies along the Caribbean coast of Panama, where decapods are especially diverse and abundant. Although a decapod assemblage consisting of both anomurans and brachyurans has already been reported from the Acquabona outcrop by De Angeli et al. [158], their local abundance was greatly underestimated by previous studies [44], possibly due to the difficulties in separating decapod remains from other shell fragments in thin sections (especially bivalves).

Table 2. Comparison between the Acquabona outcrop Upper Miocene coral boundstone and other Upper Miocene coral boundstones from other areas of the Mediterranean.

Composition of the Skeletal Assemblage (% Point-Counting)	**Coral Boundstone—Core (Acquabona)**	**Coral Boundstone—Transitional (Acquabona)**	**Coral Reef (Eratosthenes Seamount [92])**	**Coral Reef (Cyprus [91])**
Symbiont-bearing colonial corals	46	7.5	38	25
Red calcareous algae	26.5	39	32.5	35
Green calcareous algae	0.5	3.5	0	1
Large benthic foraminifera	0	1	9.5	0.5
Encrusting benthic foraminifera	8.5	3	5	24
Small benthic foraminifera	2	3	7	2
Planktic foraminifera	0	0	0	0
Mollusks	3	9.5	4	6
Echinoderms	4	9.5	3	2
Decapods	7.5	16	0.5	2.5
Sessile heterotrophs	1.5	7.5	0.5	1.5
Others	0.5	0.5	0	0.5
Autotrophs + mixotrophs	73	51	80	61.5
Heterotrophs	26.5	48.5	20	38

Based on paleogeographic reconstructions, the Acquabona reef should have been located around 35–40° N [159], which is way north of any modern coral reef of a similar size. Currently, the northernmost structures of this type are found in the Iki and Tsushima islands of Japan, at 33–34° N [10,11]. While, globally speaking, Late Miocene temperatures were close to the current ones, the Mediterranean temperatures might have been around some 5 °C above modern levels [35,160]. The present-day sea surface temperatures in the Tyrrhenian Sea off Tuscany (Figure 2) range from 24 °C during summer to 11 °C during winter [161]. Therefore, average temperatures 5 °C higher than the modern ones would make the Acquabona paleoenvironment similar or warmer than present-day Iki and Tsushima Islands (that currently range between 26.5 °C in summer and 13.5 °C in winter), and, as such, within the habitability range for corals (18 °C to 30 °C) [162,163].

Although temperature-wise, during the Late Miocene, the Acquabona area might have been suitable for the settling of corals, the detailed analysis of the outcrop reveals a more complex picture. The high degree of encrustation of the coral colonies is a prime difference between the Upper Miocene reefs of Acquabona and those of Cyprus and Eratosthenes in the Eastern Mediterranean. Indeed, in the Acquabona site, almost every colony observed in the outcrop is entirely encrusted. Sessile benthic organisms fiercely compete for space and light in modern reefs, and this is particularly true for corals and coralline algae [164,165]. Coralline algae and other sclerobionts can benefit from the cryptic microhabitats provided by corals, so much so that encrustation alone does not necessarily demonstrate that a given reef is unhealthy [148,152]. Furthermore, healthy corals are generally able to fend off coralline algae and other encrusters from their living tissues [165]. However, unhealthy or damaged corals may lose their competitive edge over secondary encrusters [165], and mass mortality events can trigger a takeover of the reef by other organisms [166]. Therefore, the pervasive presence of a diverse array of encrusters that completely covers the coral colonies suggests short-term shutdowns of the coral-dominated carbonate factory. Small environmental oscillations may have favored the temporary dominance of coralline algae and encrusting benthic foraminifera over colonial corals. Having developed at the edge of the coral ecospace, during a period of strong climatic fluctuations [31,32,36,62,68], even the slightest change may have resulted in a temporary

shutdown (or at least a remarkable reduction) of the coral-dominated carbonate factory, thus favoring the temporary dominance of more adaptable and flexible groups such as coralline algae and encrusting benthic foraminifera [149,167]. Given the high latitude, it is unlikely that these perturbations were bleaching events. Considering the ancillary assemblage, cold periods and eutrophication are both possible underlying causes. A similar pattern of pervasive encrustation can be observed also in those Mediterranean Messinian carbonate systems that feature a terminal carbonate complex (sensu Esteban [168]). This kind of deposit is typical of the early stages of evaporite deposition during the MSC and consists of oolites, evaporitic limestones, fresh- and brackish-water limestones, *Porites* reefs, serpulid accumulations, and stromatolites [168]. Compared to the Messinian coral reefs that developed before the crisis, the coral bioconstructions of the terminal complex are much richer in encrusting foraminifera (mainly nubeculariids) and microbial crusts [96,169]. This suggests that the pervasive presence of encrusters is, most likely, a proxy for stressed conditions (i.e., oscillations in nutrient availability, salinity, or a mixture of both).

Considering the overall facies distribution in the investigated Acquabona succession, a general trend toward more shallow, restricted and, arguably, more stressful conditions, occurs upwards along the succession. The transition from the coral boundstone to the coralline algal rudstone is associated with a decrease in water depth. As modern corals developed up to sea level, their demise is unlikely to have been caused by the decrease in water depth but rather by the establishment of environmental conditions too stressful for corals and suitable for the more flexible and adaptable coralline algae. A similar pattern is also present in the Upper Miocene succession of Malta, where a decline in coral abundance occurred during a shallowing upwards phase preceding the MSC [170]. The coralline algal rudstone overlying the coral boundstone is further overlain by the serpulid floatstone to packstone. Serpulids can thrive and form mass occurrences even in extremely stressful conditions, and especially in restricted settings [145,171]. Within Miocene carbonate systems, serpulids abundance often increases moving towards stressful, restricted conditions [96,146].

The serpulid facies is further overlain by the peloidal packstone to grainstone facies. The latter lacks evidence for the presence of relevant metazoan carbonate producers, probably caused by the very shallow water setting influenced by tidal excursions. In other Late Miocene Mediterranean shallow-water carbonate systems, such a dramatic reduction in the diversity of the skeletal assemblage is usually associated with the dominance of microbial carbonate like that noted in the terminal complexes [168]. In these deposits, the emergence of microbialites at the expense of metazoans is suggested to reflect a stress-driven ecosystem collapse [172–174]. Microbial structures and stromatolites have been reported by Bossio et al. [44] in the bioclastic deposits that overlay the investigated succession of Acquabona, namely the lagoonal carbonate interval and the Castelnuovo reef. However, our analysis did not indicate a relevant microbial contribution to the studied succession. The lack of a clear microbialite texture represents a relevant difference between the investigated Upper Miocene reef of the Acquabona reef and other coeval examples of the Mediterranean area. This difference could be related to the following: (a) a major competition between metazoan and carbonatogenic bacteria in comparison to other coeval Mediterranean settings [40,98,169]; (b) the higher latitude preventing abundant induced and/or influenced deposition of carbonate (i.e., not related to enzymatic control, like the controlled precipitation of the carbonate secreted by metazoan, but mediated indirectly by microbial metabolic processes or influenced by surface-specific organic molecules [175–179]). Further micro- to nano-morphological observations as well as mineralogical and biogeochemical analyses will be performed to better investigate this topic in order to elucidate the general paleoecological evolution of the metazoan/microbial bioconstructions during the MSC.

The overall trend of the lower part of the Calcare di Rosignano Formation toward more shallow and restricted marine conditions was reported also by Bossio et al. [44]. This progressive reduction in water circulation is most likely related to the overall reduction in the connectivity between the Atlantic and Mediterranean basins that occurred during

the Late Miocene. However, according to Bossio et al. [44], the Acquabona reef is overlain by the lagoonal carbonate interval, which in turn is capped by a caliche crust. This subaerial exposure surface should be related to a relative sea-level oscillation preceding the MSC [180]. Indeed, based on geometrical reconstructions, a younger carbonate system, the Castelnuovo reef, occur above the lagoonal carbonate interval and below the deposits related to the MSC [44]. However, the geometrical relationships proposed by Bossio et al. [44] can no longer be verified on the field as the entire area has been engulfed by vegetation, leaving the question up to debate.

Regardless of the timing of its final demise, the investigated Acquabona succession clearly displays the effect of environmental oscillations on a reef that shared relevant similarities with modern ones. Like present-day reefs, the Acquabona reef developed at very shallow depth and was dominated by colonial corals and coralline red algae. Similar to modern reefs growing at the fringes of the tropical zone, it was characterized by a reduced coral biodiversity and a relevant amount of heterotrophs. Therefore, the behavior of the investigated Acquabona reef can provide useful insights into how modern coral reefs located at the fringes of the symbiont-bearing colonial corals ecospace will react to environmental fluctuations. The minor oscillations recorded within the coral boundstone itself were already able to temporarily shut down carbonate production by colonial corals. The slightly stronger variations recorded upwards in the succession resulted in the complete demise of colonial corals, indicating the vulnerability of this type of coral reef.

7. Conclusions

The investigated early Messinian succession of the Acquabona quarry displays the demise of a coral reef. Sedimentologically, this is manifested as the transition from a coral boundstone with low diversity to a coralline algal rudstone (still including some rare coral fragments), followed by serpulid floatstone to packstone, and, finally, by peloidal packstone to grainstone. The reef interval probably developed in a shallow euphotic setting (possibly 20 m of water depth or less), while the overlaying intervals testify for an increasingly shallower environment characterized by progressively more restricted water circulation.

The studied succession displays significant similarities with modern reefs developed at high latitudes as it is characterized by a limited coral biodiversity and includes a relevant amount of heterotrophs (in particular crustaceans). Much like in modern oceans, the Acquabona reef displays a higher amount of heterotrophs than other reefs formed at lower latitudes and farther away from nutrient sources. Given these parallels, it is possible to consider the Acquabona succession as a useful proxy for understanding the response of coral reefs to environmental disturbances. The abundance of coral colonies pervasively encrusted by coralline algae, encrusting benthic foraminifera, and bryozoans suggests short-term, temporary shutdowns of the coral-dominated carbonate factory caused by minor environmental perturbations. The overall upward increase in carbonate producers (coralline algae at first and serpulids later) that are more flexible and adaptable than corals suggests that deteriorating environmental conditions caused the collapse of the coral factory, such an environmental degradation being most likely related to the progressive restriction of the Mediterranean circulation during the Late Miocene. These findings suggest that reefs developing at the fringes of the coral niche are inherently fragile; they can be damaged even by minor perturbations and can collapse entirely if unfavorable conditions persists for too long.

Author Contributions: Conceptualization: G.C., G.B. and O.M.B.; methodology; G.C. and O.M.B.; software; G.C., A.V. (Alberto Vimercati) and O.M.B.; validation: G.C., F.R.B., D.B. and O.M.B.; formal analysis: G.C., F.R.B., A.C., G.B., A.G., A.V. (Alessandro Vescogni), D.B. and O.M.B.; investigation: G.C., A.V. (Alberto Vimercati), F.R.B., A.C., G.B., A.G., A.V. (Alessandro Vescogni), D.B. and O.M.B.; resources: G.C. and O.M.B.; data curation: G.C., A.V. (Alberto Vimercati), F.R.B., A.C., G.B., A.G., A.V. (Alessandro Vescogni), D.B. and O.M.B.; writing-original draft preparation: G.C., A.V. (Alberto Vimercati) and O.M.B.; writing-review and editing: G.C., A.V. (Alberto Vimercati), F.R.B., A.C., G.B., A.G., A.V. (Alessandro Vescogni), D.B. and O.M.B.; visualization: G.C., A.V. (Alberto Vimercati)

and O.M.B.; supervision: G.C.; project administration: G.C. and A.C.; funding acquisition: this research received no external funding. All authors have read and agreed to the published version of the manuscript.

Funding: This research received no external funding.

Data Availability Statement: All the relevant data regarding the investigated assemblages are included into the tables of the manuscript.

Acknowledgments: The authors are grateful to the Società Paleontologica Italiana for having fostered the fruitful research environment that generated the current research and to two anonymous reviewers for the useful suggestions. Special thanks also go to Irene Cornacchia (CNRR-IGAG) for her assistance during the field work, the fruitful discussions, and the precious insights on Mediterranean paleoceanography. This research also represents a scientific contribution of the Project MIUR - Dipartimenti di Eccellenza 2023–2027.

Conflicts of Interest: The authors declare no conflicts of interest.

References

1. Hughes, T.P.; Baird, A.H.; Bellwood, D.R.; Card, M.; Connolly, S.R.; Folke, C.; Grosberg, R.; Hoegh-Guldberg, O.; Jackson, J.B.C.; Kleypas, J.; et al. Climate change, human impacts, and the resilience of coral reefs. *Science* **2003**, *301*, 929–933. [CrossRef] [PubMed]
2. Bialik, O.M.; Coletti, G.; Mariani, L.; Commissario, L.; Desbiolles, F.; Meroni, A.N. Availability and type of energy regulate the global distribution of neritic carbonates. *Sci. Rep.* **2023**, *13*, 19687. [CrossRef] [PubMed]
3. Hoegh-Guldberg, O.; Mumby, P.J.; Hooten, A.J.; Steneck, R.S.; Greenfield, P.; Gomez, E.; Harvell, C.D.; Sale, P.F.; Edwards, A.J.; Caldeira, K.; et al. Coral reefs under rapid climate change and ocean acidification. *Science* **2007**, *318*, 1737–1742. [CrossRef] [PubMed]
4. Hughes, T.P.; Kerry, J.T.; Álvarez-Noriega, M.; Álvarez-Romero, J.G.; Anderson, K.D.; Baird, A.H.; Babcock, R.C.; Beger, M.; Bellwood, D.R.; Berkelmans, R.; et al. Global warming and recurrent mass bleaching of corals. *Nature* **2017**, *543*, 373–377. [CrossRef]
5. Van Woesik, R.; Shlesinger, T.; Grottoli, A.G.; Toonen, R.J.; Vega Thurber, R.; Warner, M.E.; Marie Hulver, A.; Chapron, L.; Mclachlan, R.H.; Albright, R.; et al. Coral-bleaching responses to climate change across biological scales. *Glob. Change Biol.* **2022**, *28*, 4229–4250. [CrossRef]
6. IPCC. *Climate Change 2022: Impacts, Adaptation, and Vulnerability*; Cambridge University Press: Cambridge, UK, 2022.
7. Hughes, T.P.; Anderson, K.D.; Connolly, S.R.; Heron, S.F.; Kerry, J.T.; Lough, J.M.; Baird, A.H.; Baum, J.K.; Berumen, M.L.; Bridge, T.C.; et al. Spatial and temporal patterns of mass bleaching of corals in the Anthropocene. *Science* **2018**, *359*, 80–83. [CrossRef]
8. Oliver, J.K.; Berkelmans, R.; Eakin, C.M. Coral bleaching in space and time. In *Coral Bleaching: Patterns, Processes, Causes and Consequences*; Springer: Berlin/Heidelberg, Germany, 2018; pp. 27–49.
9. Pisapia, C.; Hochberg, E.J.; Carpenter, R. Multi-decadal change in reef-scale production and calcification associated with recent disturbances on a Lizard Island reef flat. *Front. Mar. Sci.* **2019**, *6*, 575. [CrossRef]
10. Yamano, H.; Hori, K.; Yamauchi, M.; Yamagawa, O.; Ohmura, A. Highest-latitude coral reef at Iki Island, Japan. *Coral Reefs* **2001**, *20*, 9–12.
11. Yamano, H.; Sugihara, K.; Watanabe, T.; Shimamura, M.; Hyeong, K. Coral reefs at 34 N, Japan: Exploring the end of environmental gradients. *Geology* **2012**, *40*, 835–838. [CrossRef]
12. Greenstein, B.J.; Pandolfi, J.M. Escaping the heat: Range shifts of reef coral taxa in coastal Western Australia. *Glob. Change Biol.* **2008**, *14*, 513–528. [CrossRef]
13. Harrison, P.L.; Dalton, S.J.; Carroll, A.G. Extensive coral bleaching on the world's southernmost coral reef at Lord Howe Island, Australia. *Coral Reefs* **2011**, *30*, 775. [CrossRef]
14. Price, N.N.; Muko, S.; Legendre, L.; Steneck, R.; van Oppen, M.J.H.; Albright, R.; Ang, P., Jr.; Carpenter, R.C.; Chui, A.P.Y.; Fan, T.Y.; et al. Global biogeography of coral recruitment: Tropical decline and subtropical increase. *Mar. Ecol. Prog. Ser.* **2019**, *621*, 1–17. [CrossRef]
15. Sully, S.; van Woesik, R. Turbid reefs moderate coral bleaching under climate-related temperature stress. *Glob. Change Biol.* **2020**, *26*, 1367–1373. [CrossRef] [PubMed]
16. Rosedy, A.; Ives, I.; Waheed, Z.; Syed Hussein, M.A.; Sosdian, S.; Johnson, K.; Santodomingo, N. Turbid reefs experience lower coral bleaching effects in NE Borneo (Sabah, Malaysia). *Reg. Stud. Mar. Sci.* **2023**, *68*, 103268. [CrossRef]
17. Cacciapaglia, C.; van Woesik, R. Climate-change refugia: Shading reef corals by turbidity. *Glob. Change Biol.* **2016**, *22*, 1145–1154. [CrossRef]
18. Green, R.H.; Lowe, R.J.; Buckley, M.L.; Foster, T.; Gilmour, J.P. Physical mechanisms influencing localized patterns of temperature variability and coral bleaching within a system of reef atolls. *Coral Reefs* **2019**, *38*, 759–771. [CrossRef]
19. Hammerman, N.M.; Roff, G.; Lybolt, T.; Eyal, G.; Pandolfi, J.M. Unraveling Moreton Bay reef history: An urban high-latitude setting for coral development. *Front. Ecol. Evol.* **2022**, *10*, 884850. [CrossRef]

20. Smith, L.D.; Gilmour, J.P.; Heyward, A.J. Resilience of coral communities on an isolated system of reefs following catastrophic mass-bleaching. *Coral Reefs* **2008**, *27*, 197–205. [CrossRef]
21. Woodroffe, C.D.; Brooke, B.P.; Linklater, M.; Kennedy, D.M.; Jones, B.G.; Buchanan, C.; Mleczko, R.; Hua, Q.; Zhao, J. Response of coral reefs to climate change: Expansion and demise of the southernmost Pacific coral reef. *Geophys. Res. Lett.* **2010**, *37*, L156022010. [CrossRef]
22. Graham, N.A.J.; Nash, K.L.; Kool, J.T. Coral reef recovery dynamics in a changing world. *Coral Reefs* **2011**, *30*, 283–294. [CrossRef]
23. Pisapia, C.; Burn, D.; Yoosuf, R.; Najeeb, A.; Anderson, K.D.; Pratchett, M.S. Coral recovery in the central Maldives archipelago since the last major mass-bleaching, in 1998. *Sci. Rep.* **2016**, *6*, 34720. [CrossRef] [PubMed]
24. Xie, J.Y.; Yeung, Y.H.; Kwok, C.K.; Kei, K.; Ang, P., Jr.; Chan, L.L.; Cheang, C.C.; Chow, W.K.; Qiu, J.W. Localized bleaching and quick recovery in Hong Kong's coral communities. *Mar. Pollut. Bull.* **2020**, *153*, 110950. [CrossRef] [PubMed]
25. Leinbach, S.E.; Speare, K.E.; Rossin, A.M.; Holstein, D.M.; Strader, M.E. Energetic and reproductive costs of coral recovery in divergent bleaching responses. *Sci. Rep.* **2021**, *11*, 23546. [CrossRef] [PubMed]
26. Huntington, B.; Weible, R.; Halperin, A.; Winston, M.; McCoy, K.; Amir, C.; Asher, J.; Vargas-Angel, B. Early successional trajectory of benthic community in an uninhabited reef system three years after mass coral bleaching. *Coral Reefs* **2022**, *41*, 1087–1096. [CrossRef]
27. Vessaz, F.; Marsh, C.J.; Bijoux, J.; Gendron, G.; Mason-Parker, C. Recovery trajectories of oceanic reef ecosystems following multiple mass coral bleaching events. *Mar. Biol.* **2022**, *169*, 23. [CrossRef]
28. Westphal, H.; Halfar, J.; Freiwald, A. Heterozoan carbonates in subtropical to tropical settings in the present and past. *Int. J. Earth Sci.* **2010**, *99*, 153–169. [CrossRef]
29. Pandolfi, J.M.; Kiessling, W. Gaining insights from past reefs to inform understanding of coral reef response to global climate change. *Curr. Opin. Environ. Sustain.* **2014**, *7*, 52–58. [CrossRef]
30. Tierney, J.E.; Poulsen, C.J.; Montanez, I.P.; Bhattacharya, T.; Feng, R.; Ford, H.L.; Honisch, B.; Inglis, G.N.; Petersen, S.V.; Sagoo, N.; et al. Past climates inform our future. *Science* **2020**, *370*, eaay3701. [CrossRef]
31. Miller, K.G.; Browning, J.V.; Schmelz, W.J.; Kopp, R.E.; Mountain, G.S.; Wright, J.D. Cenozoic sea-level and cryospheric evolution from deep-sea geochemical and continental margin records. *Sci. Adv.* **2020**, *6*, eaaz1346. [CrossRef]
32. Di Stefano, A.; Verducci, M.; Lirer, F.; Ferraro, L.; Iaccarino, S.M.; Hüsing, S.K.; Hilgen, F. J Paleoenvironmental conditions preceding the Messinian Salinity Crisis in the Central Mediterranean: Integrated data from the Upper Miocene Trave section (Italy). *Palaeogeogr. Palaeoclimatol. Palaeoecol.* **2010**, *297*, 37–53. [CrossRef]
33. Perrin, C.; Bosellini, F.R. Paleobiogeography of scleractinian reef corals: Changing patterns during the Oligocene–Miocene climatic transition in the Mediterranean. *Earth-Sci. Rev.* **2012**, *111*, 1–24. [CrossRef]
34. Perrin, C.; Bosellini, F.R. The Late Miocene cold spot of z-corals diversity in the Mediterranean: Patterns and causes. *Comptes. Rendus. Palevol.* **2013**, *12*, 245–255. [CrossRef]
35. Prista, G.A.; Agostinho, R.J.; Cachão, M.A. Observing the past to better understand the future: A synthesis of the Neogene climate in Europe and its perspectives on present climate change. *Open Geosci.* **2015**, *7*, 20150007. [CrossRef]
36. Flecker, R.; Krijgsman, W.; Capella, W.; de Castro Martíns, C.; Dmitrieva, E.; Mayser, J.P.; Marzocchi, A.; Modestu, S.; Ochoa, D.; Simon, D.; et al. Evolution of the late Miocene Mediterranean–Atlantic gateways and their impact on regional and global environmental change. *Earth Sci. Rev.* **2015**, *150*, 365–392. [CrossRef]
37. Steinthorsdottir, M.; Coxall, H.K.; De Boer, A.M.; Huber, M.; Barbolini, N.; Bradshaw, C.D.; Burls, N.J.; Feakins, S.J.; Gasson, E.; Henderiks, J.; et al. The Miocene: The future of the past. *Paleoceanogr. Paleoclimatology* **2021**, *36*, e2020PA004037. [CrossRef]
38. Mertz-Kraus, R.; Brachert, T.C.; Reuter, M.; Galer, S.J.G.; Fassoulas, C.; Iliopoulos, G. Late Miocene sea surface salinity variability and paleoclimate conditions in the Eastern Mediterranean inferred from coral aragonite δ18O. *Chem. Geol.* **2009**, *262*, 202–216. [CrossRef]
39. Simon, D.; Marzocchi, A.; Flecker, R.; Lunt, D.J.; Hilgen, F.J.; Meijer, P.T. Quantifying the Mediterranean freshwater budget throughout the late Miocene: New implications for sapropel formation and the Messinian Salinity Crisis. *Earth Planet. Sci. Lett.* **2017**, *472*, 25–37. [CrossRef]
40. Esteban, M. An overview of Miocene reefs from Mediterranean areas: General trends and facies models. In *Models for Carbonate Stratigraphy from Miocene Reef Complexes of Mediterranean Region*; SEPM Concepts in Sedimentology and Paleontology Series; Franseen, E.K., Estaban, M., Ward, W.C., Rouchy, J., Eds.; SEPM: Tulsa, OK, USA, 1996; Volume 5, pp. 3–53.
41. Vertino, A.; Stolarski, J.; Bosellini, F.R.; Taviani, M. Mediterranean corals through time: From Miocene to Present. In *The Mediterranean Sea: Its History and Present Challenges*; Springer: Berlin/Heidelberg, Germany, 2014; pp. 257–274.
42. Pomar, L.; Baceta, J.I.; Hallock, P.; Mateu-Vicens, G.; Basso, D. Reef building and carbonate production modes in the west-central Tethys during the Cenozoic. *Mar. Pet. Geol.* **2017**, *83*, 261–304. [CrossRef]
43. Bossio, A.; Bradley, F.; Esteban, M.; Giannelli, L.; Landini, W.; Mazzanti, R.; Mazzei, R.; Salvatorini, G. Alcuni aspetti del Miocene superiore della Val di Fine. In Proceedings of the Field Trip Guide IX Convegno della Società Paleontologica Italiana, Pisa, Italy, 3–8 October 1981; pp. 21–54.
44. Bossio, A.; Esteban, M.; Mazzanti, R.; Mazzei, R.; Salvatorini, G. Rosignano reef complex (Messinian), Livornesi Mountains, Tuscany, central Italy. In *Models for Carbonate Stratigraphy from Miocene Reef Complexes of the Mediterranean Regions*; SEPM Concepts in Sedimentology and Paleontology; Franseen, E.K., Esteban, M., Ward, W.C., Rouchy, J.M., Eds.; SEPM: Tulsa, OK, USA, 1996; Volume 5, pp. 277–294.

45. Franseen, E.K.; Esteban, M.; Ward, W.C.; Rouchy, J.M. *Models for Carbonate Stratigraphy from Miocene Reef Complexes of Mediterranean Regions*; SEPM Concepts in Sedimentology and Paleontology Series; SEPM: Tulsa, OK, USA, 1996; Volume 5, p. 391.
46. Jokiel, P.; Martinelli, F.J. The vortex model of coral reef biogeography. *J. Biogeogr.* **1992**, *19*, 449–458. [CrossRef]
47. Wood, S.; Paris, C.B.; Ridgwell, A.; Hendy, E.J. Modelling dispersal and connectivity of broadcast spawning corals at the global scale. *Glob. Ecol. Biogeogr.* **2014**, *23*, 1–11. [CrossRef]
48. Popov, S.V.; Rozanov, A.Y.; Rögl, F.; Steininger, F.F.; Shcherba, I.G.; Kovac, M. Lithological-paleogeographic maps of Paratethys. *CFS Courier Forschungsinstitut Senckenberg* **2004**, *250*, 1–46.
49. Cornacchia, I.; Agostini, S.; Brandano, M. Miocene oceanographic evolution based on the Sr and Nd isotope record of the Central Mediterranean. *Paleoceanogr. Paleoclimatology* **2018**, *33*, 31–47. [CrossRef]
50. Bialik, O.M.; Frank, M.; Betzler, C.; Zammit, R.; Waldmann, N.D. Two-step closure of the Miocene Indian Ocean Gateway to the Mediterranean. *Sci. Rep.* **2019**, *9*, 8842. [CrossRef]
51. Von der Heydt, A.; Dijkstra, H.A. Effect of ocean gateways on the global ocean circulation in the late Oligocene and early Miocene. *Paleoceanography* **2006**, *21*, PA1011. [CrossRef]
52. Mihaljević, M.; Korpanty, C.; Renema, W.; Welsh, K.; Pandolfi, J.M. Identifying patterns and drivers of coral diversity in the Central Indo-Pacific marine biodiversity hotspot. *Paleobiology* **2017**, *43*, 343–364. [CrossRef]
53. Vogt-Vincent, N.S.; Mitarai, S.; Johnson, H.L. High-frequency variability dominates potential connectivity between remote coral reefs. *Limnol. Oceanogr.* **2023**, *68*, 2733–2748. [CrossRef]
54. Harzhauser, M.; Kroh, A.; Mandic, O.; Piller, W.E.; Göhlich, U.; Reuter, M.; Berning, B. Biogeographic responses to geodynamics: A key study all around the Oligo–Miocene Tethyan Seaway. *Zoologischer Anzeiger-A J. Comp.Zool.* **2007**, *246*, 241–256. [CrossRef]
55. Hüsing, S.K.; Zachariasse, W.-J.; van Hinsbergen, D.J.J.; Krijgsman, W.; Inceöz, M.; Harzhauser, M.; Mandic, O.; Kroh, A. Oligocene-Miocene basin evolution in SE Anatolia, Turkey: Constraints on the closure of the eastern Tethys gateway. In *Collision and Collapse at the Africa-Arabia–Eurasia Subduction Zone*; Van Hinsbergen, D.J.J., Edwards, M.A., Govers, R., Eds.; Geological Society of London: London, UK, 2009; Volume 311, pp. 107–132.
56. Simon, D.; Palcu, D.; Meijer, P.; Krijgsman, W. The sensitivity of middle Miocene paleoenvironments to changing marine gateways in Central Europe. *Geology* **2019**, *47*, 35–38. [CrossRef]
57. Krijgsman, W.; Palcu, D.V.; Andreetto, F.; Stoica, M.; Mandic, O. Changing seas in the late Miocene Northern Aegean: A Paratethyan approach to Mediterranean basin evolution. *Earth-Sci. Rev.* **2020**, *210*, 103386. [CrossRef]
58. Cornacchia, I.; Munnecke, A.; Brandano, M. The potential of carbonate ramps to record C-isotope shifts: Insights from the upper Miocene of the Central Mediterranean area. *Lethaia* **2021**, *54*, 73–89. [CrossRef]
59. Harzhauser, M.; Mandic, O.; Zuschin, M. Changes in Paratethyan marine molluscs at the Early/Middle Miocene transition: Diversity, palaeogeography and palaeoclimate. *Acta Geol. Pol.* **2003**, *53*, 323–339.
60. Monegatti, P.; Raffi, S. The Messinian marine molluscs record and the dawn of the eastern Atlantic biogeography. *Palaeogeogr. Palaeoclimatol. Palaeoecol.* **2010**, *297*, 1–11. [CrossRef]
61. Zachos, J.; Pagani, M.; Sloan, L.; Thomas, E.; Billups, K. Trends, rhythms, and aberrations in global climate 65 Ma to present. *Science* **2001**, *292*, 686–693. [CrossRef]
62. Herbert, T.D.; Lawrence, K.T.; Tzanova, A.; Peterson, L.C.; Caballero-Gill, R.; Kelly, C.S. Late Miocene global cooling and the rise of modern ecosystems. *Nat. Geosci.* **2016**, *9*, 843–847. [CrossRef]
63. Bruch, A.A.; Utescher, T.; Mosbrugger, V. Precipitation patterns in the Miocene of Central Europe and the development of continentality. *Palaeogeogr. Palaeoclimatol. Palaeoecol.* **2011**, *304*, 202–211. [CrossRef]
64. Bosellini, F.R.; Perrin, C. Estimating Mediterranean Oligocene–Miocene sea-surface temperatures: An approach based on coral taxonomic richness. *Palaeogeogr. Palaeoclimatol. Palaeoecol.* **2008**, *258*, 71–88. [CrossRef]
65. Agiadi, K.; Hohmann, N.; Gliozzi, E.; Thivaiou, D.; Bosellini, F.R.; Taviani, M.; Bianucci, G.; Collareta, A.; Londeix, L.; Faranda, C.; et al. Late Miocene transformation of Mediterranean Sea biodiversity. *Sci. Adv.* **2024**, *10*, eadp1134. [CrossRef]
66. Filippelli, G.M.; Sierro, F.J.; Flores, J.A.; Vázquez, A.; Utrilla, R.; Pérez-Folgado, M.; Latimer, J.C. A sediment–nutrient–oxygen feedback responsible for productivity variations in Late Miocene sapropel sequences of the western Mediterranean. *Palaeogeogr. Palaeoclimatol. Palaeoecol.* **2003**, *190*, 335–348. [CrossRef]
67. Bulian, F.; Kouwenhoven, T.J.; Jiménez-Espejo, F.J.; Krijgsman, W.; Andersen, N.; Sierro, F.J. Impact of the Mediterranean-Atlantic connectivity and the late Miocene carbon shift on deep-sea communities in the Western Alboran Basin. *Palaeogeogr. Palaeoclimatol. Palaeoecol.* **2022**, *589*, 110841. [CrossRef]
68. Diester-Haass, L.; Billups, K.; Emeis, K.C. Late Miocene carbon isotope records and marine biological productivity: Was there a (dusty) link? *Paleoceanography* **2006**, *21*, PA4216. [CrossRef]
69. Böhme, M.; Ilg, A.; Winklhofer, M. Late Miocene "washhouse" climate in Europe. *Earth Planet. Sci. Lett.* **2008**, *275*, 393–401. [CrossRef]
70. Chevalier, J.P. Recherches sur les madréporaires et les formations récifales miocènes de la Méditerranée occidentale. *Mémoires Société Géologique Fr.* **1962**, *93*, 1–558.
71. Santisteban, G.; Taberner, C. Sedimentary models of siliciclastic deposits and coral reefs inter-relation. In: Doyle, L.J.; Roberts, H.H. (Eds.), Carbonate–Clastic Transitions. *Dev. Sedimentol.* **1988**, *42*, 35–77.
72. Martin, J.M.; Braga, J.C.; Rivas, P. Coral successions in Upper Tortonian reefs in SE Spain. *Lethaia* **1989**, *22*, 271–286. [CrossRef]

73. Braga, J.C.; Martin, J.M.; Alcala, B. Coral reefs in coarse-terrigenous sedimentary environments (Upper Tortonian, Granada Basin, southern Spain). *Sediment. Geol.* **1990**, *66*, 135–150. [CrossRef]
74. Vennin, E.; Rouchy, J.M.; Chaix, C.; Blanc-Valleron, M.; Caruso, A.; Rommevau, V. Paleoecological constraints on reef-coral morphologies in the Tortonian–early Messinian of the Lorca basin, SE Spain. *Palaeogeogr. Palaeoclimatol. Palaeoecol.* **2004**, *213*, 163–185. [CrossRef]
75. Pomar, L. Reef geometries, erosion surfaces and high-frequency sea-level changes, upper Miocene reef complex, Mallorca, Spain. *Sedimentology* **1991**, *38*, 243–269. [CrossRef]
76. Pomar, L.; Ward, W.C.; Green, D.G. Upper Miocene reef complex of the Llucmajor area, Mallorca, Spain. In *Models for Carbonate Stratigraphy from Miocene Reef Complexes of Mediterranean Regions*; Franseen, E.K., Esteban, M., Ward, W.C., Rouchy, J.-M., Eds.; SEPM Concepts in Sedimentology and Paleontology Series; SEPM: Tulsa, OK, USA, 1996; Volume 5, pp. 191–225.
77. Saint-Martin, J.P. Les formations récifales coralliennes du Miocène supérieur d'Algérie et du Maroc. Aspects paléoécologiques et paléogéographiques. Doctoral Thesis, Université Aix-Marseille I, Marseille, France, 1987.
78. Pedley, H.M.; Grasso, M. *Upper Miocene peri-Tyrrhenian Reefs in the Calabrian Arc: Sedimentological, Tectonic and Palaeogeographic Implications*; Géologie Méditerranéenne: Marseille, France, 1994; Volume 21, pp. 123–136.
79. Pedley, H.M.; Grasso, M. *The Sedimentology of Late Miocene Peri-Tyrrhenian Reefs in Sicily and Calabria and Their Tectonic Implications*; IAS Ischia94; Éditions de l'Université de Provence: Ischia, Italy, 1994; pp. 322–323.
80. Grasso, M.; Lentini, F.; Pedley, H.M. Late Tortonian–lower Messinian (Miocene) palaeogeography of SE Sicily: Information from two new formations of the Sortino Group. *Sediment. Geol.* **1982**, *32*, 279–300. [CrossRef]
81. Pedley, H.M. The petrology and palaeoenvironment of the Sortino Group (Miocene) of SE Sicily: Evidence for periodic emergence. *J. Geol. Soc. Lond.* **1983**, *140*, 335–350. [CrossRef]
82. Pedley, H.M. Miocene reef facies of the Pelagian region (central Mediterranean). In *Models for Carbonate Stratigraphy from Miocene Reef Complexes of Mediterranean Regions*; Franseen, E.K., Esteban, M., Ward, W.C., Rouchy, J.-M., Eds.; SEPM Concepts in Sedimentology and Paleontology Series; SEPM: Tulsa, OK, USA, 1996; Volume 5, pp. 247–259.
83. Pedley, H.M. Miocene bioherms and associated structures in the Upper Coralline limestone of the Maltese Islands: Their lithification and palaeoenvironment. *Sedimentology* **1979**, *26*, 577–591. [CrossRef]
84. Pedley, H.M. Miocene reef distributions and their associations in the central Mediterranean region: An overview. In *Models for Carbonate Stratigraphy from Miocene Reef Complexes of Mediterranean Regions*; Franseen, E.K., Esteban, M., Ward, W.C., Rouchy, J.-M., Eds.; SEPM Concepts in Sedimentology and Paleontology Series; SEPM: Tulsa, OK, USA, 1996; Volume 5, pp. 73–87.
85. Grasso, M.; Pedley, H.M. The Pelagian Islands: A new geological interpretation from sedimentological and tectonic studies and its bearing on the evolution of the Central Mediterranean Sea (Pelagian Block). *Geol. Romana* **1985**, *24*, 13–34.
86. Di Credico, N.; Fravega, P.; Giammarino, S.; Piazza, M.; Vannucci, G. Algal assemblages of Cala Pisana Member, Lampedusa Formation (Late Miocene, Lampedusa Island). *Boll. Acc. Gioenia Sci. Nat* **2004**, *37*, 217–243.
87. Baron-Szabo, R. Taxonomy and paleoecology of Late Miocene corals of NW-Crete (Gramvoţssa, Roka- and Koukounaras-Fms.). *Berl. Geowiss. Abh.* **1995**, *E16*, 569–577.
88. Brachert, T.C.; Reuter, M.; Felis, T.; Kroeger, K.F.; Lohmann, G.; Micheels, A.; Fassoulas, C. Porites corals from Crete (Greece) open a window into Late Miocene (10 MA) seasonal and interannual climate variability. *Earth Planet. Sci. Lett.* **2006**, *245*, 81–94. [CrossRef]
89. Hayward, A.B.; Robertson, A.H.F.; Scoffin, T.P. Miocene patch reefs from a Mediterranean marginal terrigenous setting in southwest Turkey. In *Models for Carbonate Stratigraphy from Miocene Reef Complexes of Mediterranean Regions: SEPM Concepts in Sedimentology and Paleontology*; Franseen, E.K., Esteban, M., Ward, W.C., Rouchy, J.-M., Eds.; SEPM (Society for Sedimentary Geology): Tulsa, OK, USA, 1996; Volume 5, pp. 317–332.
90. Follows, E.J.; Robertson, A.H.F.; Scoffin, T.P. Tectonic controls on Miocene reefs and related carbonate facies in Cyprus. In *Models for Carbonate Stratigraphy from Miocene Reef Complexes of Mediterranean Regions*; SEPM Concepts in Sedimentology and Paleontology Series; Franseen, E.K., Esteban, M., Ward, W.C., Rouchy, J.-M., Eds.; SEPM: Tulsa, OK, USA, 1996; Volume 5, pp. 295–315.
91. Coletti, G.; Balmer, E.M.; Bialik, O.M.; Cannings, T.; Kroon, D.; Robertson, A.H.; Basso, D. Microfacies evidence for the evolution of Miocene coral-reef environments in Cyprus. *Palaeogeogr. Palaeoclimatol. Palaeoecol.* **2021**, *584*, 110670. [CrossRef]
92. Coletti, G.; Basso, D.; Betzler, C.; Robertson, A.H.; Bosio, G.; El Kateb, A.; Foubert, A.; Meilijson, A.; Spezzaferri, S. Environmental evolution and geological significance of the Miocene carbonates of the Eratosthenes Seamount (ODP Leg 160). *Palaeogeogr. Palaeoclimatol. Palaeoecol.* **2019**, *530*, 217–235. [CrossRef]
93. Coletti, G.; Basso, D. Coralline algae as depth indicators in the Miocene carbonates of the Eratosthenes Seamount (ODP Leg 160, Hole 966F). *Geobios* **2020**, *60*, 29–46. [CrossRef]
94. Hladil, J.; Otava, J.; Galle, A. Oligocene carbonate buildups of the Sirt Basin, Libya. In *The Geology of Libya*; Salem, M.J., Hammuda, O.S., Eliagoubi, B.A., Eds.; Elsevier: Amsterdam, The Netherlands, 1991; Volume 4, pp. 1401–1420.
95. Tomassetti, L.; Bosellini, F.R.; Brandano, M. Growth and demise of a Burdigalian coral bioconstruction on a granite rocky substrate (Bonifacio Basin, southeastern Corsica). *Facies* **2013**, *59*, 703–716. [CrossRef]
96. Riding, R.; Martin, J.M.; Braga, J.C. Coral-stromatolite reef framework, upper Miocene, Almería, Spain. *Sedimentology* **1991**, *38*, 799–818. [CrossRef]
97. Martin, J.M.; Braga, J.C. Messinian events in the Sorbas Basin in southeastern Spain and their implications in the recent history of the Mediterranean. *Sediment. Geol.* **1994**, *90*, 257–268. [CrossRef]

98. Braga, J.C.; Martin, J.M. Geometries of reef advance in response to relative sea-level changes in a Messinian (uppermost Miocene) fringing reef (Cariatiz reef, Sorbas Basin, SE Spain). *Sediment. Geol.* **1996**, *107*, 61–81. [CrossRef]
99. Martin, J.M.; Braga, J.C.; Riding, R. Late Miocene Halimeda algal–microbial segment reefs in the marginal Mediterranean Sorbas basin, Spain. *Sedimentology* **1997**, *44*, 441–456. [CrossRef]
100. Brachert, T.C.; Hultzsch, N.; Knoerich, A.C.; Krautworst, U.M.R.; Stückrad, O.M. Climatic signatures in shallow-water carbonates: High-resolution stratigraphic markers in structurally controlled carbonate buildups (Late Miocene, southern Spain). *Palaeogeogr. Palaeoclimatol. Palaeoecol.* **2001**, *175*, 211–237. [CrossRef]
101. Brachert, T.C.; Krautworst, U.M.R.; Stueckrad, O.M. Tectono-climatic evolution of a Neogene intramontane basin (Late Miocene Carboneras subbasin, southeast Spain): Revelations from basin mapping and biofacies analysis. *BasinRes.* **2002**, *14*, 503–521. [CrossRef]
102. Saint-Martin, J.P.; Cornée, J.J.; Muller, J. Nouvelles données sur le système de plate-forme carbonatée du Messinien des environs d'Oran (Algérie). Consé- quences. *Comptes Rendus de l'Académie des Sciences de Paris, Série IIA* **1995**, *320*, 837–843.
103. Barrier, P.; Cauquil, E.; Raffi, S.; Russo, A.; Tran Van Huu, M. Signification du plus septentrional des récifs messiniens à Algues et Porites connus en Méditerranée (Vigoleno, Piacenza, Italie). In *Interim Colloquium Regional Committee of Mediterranean Neogene Stratigraphy*; IGCP 343; Université de Provence Centre Saint Charles: Marseille, France, 1994; pp. 2–3.
104. Russo, A.; Artoni, A.; Scarponi, D.; Serventi, P. Coral-algal Reef Complex of Vigoleno, Piacenza, Northern Italy. *IOP Conf. Ser. Earth Environ. Sci.* **2017**, *95*, 032034. [CrossRef]
105. Danese, E. Upper Miocene carbonate ramp deposits from the southermost part of Maiella Mountain (Abruzzo), Central Italy. *Facies* **1999**, *41*, 41–54. [CrossRef]
106. Bosellini, F.R.; Russo, A.; Vescogni, A. Messinian reef-building assemblages of the Salento Peninsula (southern Italy): Palaeo-bathymetric and palaeoclimatic significance. *Palaeogeogr. Palaeoclimatol. Palaeoecol.* **2001**, *175*, 7–26. [CrossRef]
107. Bosellini, F.R.; Russo, A.; Vescogni, A. The Messinian reef complex of the Salento Peninsula (Southern Italy): Stratigraphy, facies and paleoenvironmental interpretation. *Facies* **2002**, *47*, 91–112. [CrossRef]
108. Bosence, D.W.J.; Pedley, H.M. Sedimentology and palaeoecology of a Miocene coralline algal biostrome from the Maltese islands. *Palaeogeogr. Palaeoclimatol. Palaeoecol.* **1982**, *38*, 9–43. [CrossRef]
109. Grasso, M.; Pedley, H.M. The sedimentology and development of Terravecchia Formation carbonates (Upper Miocene) of North central Sicily: Possible eustatic influence on facies development. *Sediment. Geol.* **1988**, *57*, 131–149. [CrossRef]
110. Grasso, M.; Pedley, H.M. Palaeoenvironment of the Upper Miocene coral build-ups along the northern margins of the Caltanisetta Basin (Central Sicily). In *Regressive Pleistocene Sequence near Gravina in Puglia, Southern Italy: Sedimentological and Palaeoecological Analyses, Proceedings of the 3° Simposio di Ecologia e Paleoecologia delle Comunità Bentoniche, Catania-Taormina, Italy, 12–16 October 1985*; Università di Catania; Catania, Italy, 1989; pp. 373–389.
111. Pedley, H.M.; Grasso, M. A model for the Late Miocene reef-tripolaceous associations of Sicily and its relevance to aberrant growth-forms and reduced biological diversity within the Palaeomediterranean. In *Interim Colloquium Regional Committee of Mediterranean Neogene Stratigraphy*; IGCP 343; Université de Provence Centre Saint Charles: Marseille, France, 1994; p. 47.
112. Saint-Martin, J.P. *Messinian coral reefs of western Orania, Algeria. InModels for Carbonate Stratigraphy from Miocene Reef Complexes of Mediterranean Regions*; Franseen, E.K., Esteban, M., Ward, W.C., Rouchy, J.-M., Eds.; SEPM Concepts in Sedimentology and Paleontology Series; SEPM: Tulsa, OK, USA, 1996; Volume 5, pp. 239–246.
113. Saint-Martin, J.P. Implications de la présence de mud-mounds microbiens au Messinien (Sicile, Italie). *Comptes Rendus de l'Académie des Sciences de Paris, Série IIA* **2001**, *332*, 527–534.
114. Biely, A.; Chevalier, J.P. Présence de scléractiniaires dans le Miocène inférieur de la Tunisie septentrionale. Travaux de Géologie Tunisienne n° 8. *Notes Serv. Géologique* **1972**, *40*, 55–68.
115. Buchbinder, B. Middle and Upper Miocene reefs and carbonate platforms in Israel. In *Models for Carbonate Stratigraphy from Miocene Reef Complexes of Mediterranean Regions: SEPM Concepts in Sedimentology and Paleontology*; Franseen, E.K., Esteban, M., Ward, W.C., Rouchy, J.-M., Eds.; SEPM: Tulsa, OK, USA, 1996; Volume 5, pp. 333–345.
116. Meilijson, A.; Hilgen, F.; Sepúlveda, J.; Steinberg, J.; Fairbank, V.; Flecker, R.; Waldmann, N.D.; Spaulding, S.A.; Bialik, O.M.; Boudinot, F.G.; et al. Chronology with a pinch of salt: Integrated stratigraphy of Messinian evaporites in the deep Eastern Mediterranean reveals long-lasting halite deposition during Atlantic connectivity. *Earth-Sci. Rev.* **2019**, *194*, 374–398. [CrossRef]
117. Garcia-Castellanos, D.; Villaseñor, A. Messinian salinity crisis regulated by competing tectonics and erosion at the Gibraltar arc. *Nature* **2011**, *480*, 359–363. [CrossRef]
118. Lozar, F.; Violanti, D.; Pierre, F.D.; Bernardi, E.; Cavagna, S.; Clari, P.; Irace, A.; Martinetto, E.; Trenkwalder, S. Calcareous nannofossils and foraminifers herald the Messinian salinity crisis: The Pollenzo section (Alba, Cuneo; NW Italy). *Geobios* **2010**, *43*, 21–32. [CrossRef]
119. Pérez-Asensio, J.N.; Aguirre, J.; Schmiedl, G.; Civis, J. Messinian paleoenvironmental evolution in the lower Guadalquivir Basin (SW Spain) based on benthic foraminifera. *Palaeogeogr. Palaeoclimatol. Palaeoecol.* **2012**, *326*, 135–151. [CrossRef]
120. Carnevale, G.; Gennari, R.; Lozar, F.; Natalicchio, M.; Pellegrino, L.; Dela Pierre, F. Living in a deep desiccated Mediterranean Sea: An overview of the Italian fossil record of the Messinian salinity crisis. *Boll. Della Soc. Paleontol. Ital.* **2019**, *58*, 109–140.
121. Agiadi, K.; Hohmann, N.; Gliozzi, E.; Thivaiou, D.; Bosellini, F.R.; Taviani, M.; Bianucci, G.; Collareta, A.; Londeix, L.; Faranda, C.; et al. The marine biodiversity impact of the Late Miocene Mediterranean salinity crisis. *Science* **2024**, *385*, 986–991. [CrossRef]

122. Agiadi, K.; Hohmann, N.; Gliozzi, E.; Thivaiou, D.; Bosellini, F.R.; Taviani, M.; Bianucci, G.; Collareta, A.; Londeix, L.; Faranda, C.; et al. A revised marine fossil record of the Mediterranean before and after the Messinian Salinity Crisis. *Earth Syst. Sci. Data* **2024**, *16*, 4767–4775. [CrossRef]
123. Bossio, A.; Costantini, A.; Lazzarotto, A.; Liotta, D.; Mazzanti, R.; Mazzei, R.; Salvatorini, G.; Sandrelli, F. Rassegna delle conoscenze sulla stratigrafia del neoautoctono toscano. *Mem. Soc. Geol. Ital.* **1993**, *49*, 17–98.
124. Martini, I.P.; Sagri, M. Tecto-sedimentary characteristic of Late Miocene-Quaternary extensional basins of the Northern Apennines, Italy. *Earth Sci. Rev.* **1993**, *34*, 197–233. [CrossRef]
125. Doglioni, C.; Gueguen, E.; Harabagli, P.; Mongelli, E. On the origin of west-directed subduction zones and applications to the western Mediterranean. In *The Mediterranean Basins: Tertiary Extension within the Alpine Orogen*; Durand, B., Jolivet, L., Horvath, E., Siranne, M., Eds.; Geological Society: London, UK, 1999; Volume 156, pp. 541–561.
126. Mazzanti, R.; Bossio, A.; Cascella, A.; Foresi, M.; Mazzei, R.; Salvatorini, G.; Putignano, M.L. *Note Illustrative della Carta Geologica d'Italia alla scala 1: 50.000, Foglio 284 Rosignano Marittimo*; Servizio Geologico d'Italia; ISPRA: Roma, Italy, 2016; 189p.
127. Fravega, P.; Piazza, M.; Vannucci, G. Nongeniculate coralline algae associations from the Calcare di Rosignano Formation, lower Messinian, Tuscany (Italy). In *Studies on Ecology and Paleoecology of Benthic Communities*; Matteucci, R., Ed.; Bollettino della Società Paleontologica Italiana: Modena, Italy, 1994; Volume 2, pp. 127–140.
128. Bartoletti, E.; Giannelli, L.; Mazzanti, R.; Mazzei, R.; Salvatorini, G.; Sanesi, G.; Squarci, P. Carta Geologica del Comune di Rosignano Marittimo (Provincia di Livorno), Scala 1:25000. SELCA: Firenze, Italy, 1983.
129. Wentworth, C.K. A scale of grade and class terms for clastic sediments. *J. Geol.* **1922**, *30*, 377–392. [CrossRef]
130. Dunham, R.J. Classification of carbonate rocks according to depositional texture. In *Classification of Carbonate Rocks*; Ham, W.E., Ed.; American Association of Petroleum Geologist: Tulsa, OK, USA, 1962; Volume 1, pp. 108–121.
131. Embry, A.F.; Klovan, J.E. A Late Devonian reef tract on Northeastern Banks Island, NWT. *Bull. Can. Pet. Geol.* **1971**, *19*, 730–781.
132. Lokier, S.W.; Al Junaibi, M. The petrographic description of carbonate facies: Are we all speaking the same language? *Sedimentology* **2016**, *63*, 1843–1885. [CrossRef]
133. Flügel, E.; Munnecke, A. *Microfacies of Carbonate Rocks: Analysis, Interpretation and Application*; Springer: Berlin/Heidelberg, Germany, 2010; p. 2004.
134. Mariani, L.; Coletti, G.; Bosio, G.; Vicens, G.M.; Ali, M.; Cavallo, A.; Mittempergher, S.; Malinverno, E. Tectonically-controlled biofacies distribution in the Eocene Foraminiferal Limestone (Pag, Croatia): A quantitative-based palaeontological analysis. *Sediment. Geol.* **2024**, *472*, 106743. [CrossRef]
135. Riding, R. Structure and composition of organic reefs and carbonate mud mounds: Concepts and categories. *Earth-Sci. Rev.* **2002**, *58*, 163–231. [CrossRef]
136. Capella, W.; Flecker, R.; Hernández-Molina, F.J.; Simon, D.; Meijer, P.T.; Rogerson, M.; Sierro, F.J.; Krijgsman, W. Mediterranean isolation preconditioning the earth system for late Miocene climate cooling. *Sci. Rep.* **2019**, *9*, 3795. [CrossRef]
137. Braga, J.C.; Vescogni, A.; Bosellini, F.R.; Aguirre, J. Coralline algae (Corallinales, Rhodophyta) in western and central Mediterranean Messinian reefs. *Palaeogeogr. Palaeoclimatol. Palaeoecol.* **2009**, *275*, 113–128. [CrossRef]
138. Pomar, L. Types of carbonate platforms: A genetic approach. *Basin Res.* **2001**, *13*, 313–334. [CrossRef]
139. Hallock, P.; Glenn, E.C. Larger foraminifera: A tool for paleoenvironmental analysis of Cenozoic carbonate depositional facies. *Palaios* **1986**, *1*, 55–64. [CrossRef]
140. Dabrio, C.J.; Esteban, M.; Martin, J.M. The coral reef of Nijar, Messinian (Uppermost Miocene), Almeria Province, S.E. Spain. *Jour. Sed. Pet.* **1981**, *51*, 521–539.
141. Saint-Martin, J.P. Les formations récifales coralliennes du Miocène supérieur d'Algérie et du Maroc. *Mém. Mus. Nat. Hist. Nat.* **1990**, *56*, 1–366.
142. Basso, D. Deep rhodolith distribution in the Pontian Islands, Italy: A model for the paleoecology of a temperate sea. Palaeogeography, Palaeoclimatology. *Palaeoecology* **1998**, *137*, 173–187. [CrossRef]
143. Ten Hove, H.A. Different causes of mass occurrence in serpulids. *Biol. Syst. Colon. Org.* **1979**, *11*, 281–298.
144. Bianchi, C.N. Present-day serpulid reefs, with reference to an on-going research project on *Ficopomatus enigmaticus*. *Pubblications Serv. Géologique Luxemb.* **1995**, *29*, 61–65.
145. Bianchi, C.N.; Morri, C. The battle is not to the strong: Serpulid reefs in the lagoon of Orbetello (Tuscany, Italy). *Estuar. Coast. Shelf Sci.* **2001**, *53*, 215–220. [CrossRef]
146. Piller, W.E.; Harzhauser, M. *Nubecularia*-coralline algal-serpulid-microbial bioherms of the Paratethys Sea—Distribution and paleoecological significance (upper Serravallian, upper Sarmatian, Middle Miocene). *Geobiology* **2024**, *22*, e125902024. [CrossRef]
147. Plaziat, J.C.; Perrin, C. Multikilometer-sized reefs built by foraminifera (*Solenomeris*) from the early Eocene of the Pyrenean domain (S. France, N. Spain): Palaeoecologic relations with coral reefs. *Palaeogeogr. Palaeoclimatol. Palaeoecol.* **1992**, *96*, 195–231. [CrossRef]
148. Bosellini, F.R.; Papazzoni, C.A. Palaeoecological significance of coral-encrusting foraminiferan associations: A case-study from the Upper Eocene of northern Italy. *Acta Palaeontol. Pol.* **2003**, *48*, 279–292.
149. Coletti, G.; Commissario, L.; Mariani, L.; Bosio, G.; Desbiolles, F.; Soldi, M.; Bialik, O.M. Palaeocene to Miocene southern Tethyan carbonate factories: A meta-analysis of the successions of South-western and Western Central Asia. *Depos. Rec.* **2022**, *8*, 1031–1054. [CrossRef]

150. Granier, B.R. Reassessment of Iberopora bodeuri, a primitive plurilocular calcareous encrusting foraminifer from the "Upper Jurassic" (including Berriasian) carbonate platforms of the northern and central Tethys. *Cretac. Res.* **2024**, *155*, 105782. [CrossRef]
151. Prager, E.J.; Ginsburg, R.N. Carbonate nodule growth on Florida's outer shelf and its implications for fossil interpretations. *Palaios* **1989**, *4*, 310–317. [CrossRef]
152. Walker, S.E.; Parsons-Hubbard, K.; Richardson-White, S.; Brett, C.; Powell, E. Alpha and beta diversity of encrusting foraminifera that recruit to long-term experiments along a carbonate platform-to-slope gradient: Paleoecological and paleoenvironmental implications. *Palaeogeogr. Palaeoclimatol. Palaeoecol.* **2011**, *312*, 325–349. [CrossRef]
153. Strathearn, G.E. *Homotrema rubrum*: Symbiosis identified by chemical and isotopic analyses. *Palaios* **1986**, *1*, 48–54. [CrossRef]
154. Leutenegger, S. Symbiosis in benthic foraminifera; specificity and host adaptations. *J. Foraminifer. Res.* **1984**, *14*, 16–35. [CrossRef]
155. Tichenor, H.R.; Lewis, R.D. Distribution of Encrusting Foraminifera At San Salvador, Bahamas: A Comparison by Reef Types and Onshore− offshore Zonation. *J. Foraminifer. Res.* **2018**, *48*, 373–387. [CrossRef]
156. Van der Meij, S.E.; Bravo, H.; Scholten, Y.J.; Dromard, C.R. Host use of the elkhorn coral crab *Domecia acanthophora* (Brachyura: Domeciidae), with a phylogeny of the genus. *Cahiers Biologie Marine* **2022**, *63*, 239–246.
157. Abele, L.G. Species diversity of decapod crustaceans in marine habitats. *Ecology* **1974**, *55*, 156–161. [CrossRef]
158. De Angeli, A.; Garassino, A.; Pasini, G. New report of the coral-associated decapods from the early Messinian (Late Miocene) of Acquabona, Rosignano Marittimo (Toscana, Italy). *Nat. Hist. Sci.* **2011**, *152*, 107–122. [CrossRef]
159. Dercourt, J.; Gaetani, M.; Vrielynk, B.; Barrier, E.; Biju-Duval, B.; Brunet, M.F.; Cadet, J.P.; Crasquin, S.; Sandulescu, M. *Atlas Peri-Tethys—Palaeogeographical Maps*; CCGM/CGMW; Gauthier-Villars: Paris, France, 2000.
160. Mosbrugger, V.; Utescher, T.; Dilcher, D.L. Cenozoic continental climatic evolution of Central Europe. *Proc. Natl. Acad. Sci. USA* **2005**, *102*, 14964–14969. [CrossRef] [PubMed]
161. Pellegrini, P.F.; Bucci, M.; Tommasini, M.; Innocenti, M. Monthly averages of sea surface temperature. *Int. J. Remote Sens.* **2006**, *27*, 2519–2539. [CrossRef]
162. Veron, J.E.N. *Corals of Australia and the IndoPacific*; Angus and Robertson: London, UK; Sydney, Australia, 1986.
163. Hoegh-Guldberg, O. Climate change, coral bleaching and the future of the world's coral reefs. *Mar. Freshw. Res.* **1999**, *50*, 839–866. [CrossRef]
164. Benzoni, F.; Basso, D.; Caragnano, A.; Rodondi, G. *Hydrolithon* spp. (Rhodophyta, Corallinales) overgrow live corals (Cnidaria, Scleractinia) in Yemen. *Mar. Biol.* **2011**, *158*, 2419–2428. [CrossRef]
165. Barott, K.L.; Williams, G.J.; Vermeij, M.J.; Harris, J.; Smith, J.E.; Rohwer, F.L.; Sandin, S.A. Natural history of coral− algae competition across a gradient of human activity in the Line Islands. *Mar. Ecol. Prog. Ser.* **2012**, *460*, 1–12. [CrossRef]
166. McCook, L.; Jompa, J.; Diaz-Pulido, G. Competition between corals and algae on coral reefs: A review of evidence and mechanisms. *Coral reefs* **2001**, *19*, 400–417. [CrossRef]
167. Lokier, S.W.; Wilson, M.E.; Burton, L.M. Marine biota response to clastic sediment influx: A quantitative approach. *Palaeogeogr. Palaeoclimatol. Palaeoecol.* **2009**, *281*, 25–42. [CrossRef]
168. Esteban, M. Significance of the Upper Miocene coral reefs of the western Mediterranean. *Palaeogeogr. Palaeoclimatol. Palaeoecol.* **1979**, *29*, 169–188. [CrossRef]
169. Vescogni, A.; Guido, A.; Cipriani, A.; Gennari, R.; Lugli, F.; Lugli, S.; Manzi, V.; Reghizzi, M.; Roveri, M. Palaeoenvironmental setting and depositional model of upper Messinian microbialites of the Salento Peninsula (Southern Italy): A central Mediterranean Terminal Carbonate Complex. *Palaeogeogr. Palaeoclimatol. Palaeoecol.* **2022**, *595*, 110970. [CrossRef]
170. Bialik, O.M.; Zammit, R.; Micallef, A. Architecture and sequence stratigraphy of the Upper Coralline Limestone formation, Malta—Implications for Eastern Mediterranean restriction prior to the Messinian Salinity Crisis. *Depos. Rec.* **2021**, *7*, 256–270. [CrossRef] [PubMed]
171. Cirilli, S.; Iannace, A.; Jadoul, F.; Zamparelli, V. Microbial–serpulid build-ups in the Norian–Rhaetian of the Western Mediterranean area: Ecological response of shelf margin communities to stressed environments. *Terra Nova* **1999**, *11*, 195–202. [CrossRef]
172. Schubert, J.K.; Bottjer, D.J. Early Triassic stromatolites as post-mass extinction disaster forms. *Geology* **1992**, *20*, 883–886. [CrossRef]
173. Whalen, M.T.; Day, J.; Eberli, G.P.; Homewood, P.W. Microbial carbonates as indicators of environmental change and biotic crises in carbonate systems: Examples from the Late Devonian, Alberta basin, Canada. *Palaeogeogr. Palaeoclimatol. Palaeoecol.* **2002**, *181*, 127–151. [CrossRef]
174. Meilijson, A.; Bialik, O.M.; Benjamini, C. Stromatolitic biotic systems in the mid-Triassic of Israel—A product of stress on an epicontinental margin. *Palaeogeogr. Palaeoclimatol. Palaeoecol.* **2015**, *440*, 696–711. [CrossRef]
175. Guido, A.; Vescogni, A.; Mastandrea, A.; Demasi, F.; Tosti, F.; Naccarato, A.; Tagarelli, A.; Russo, F. Characterization of the micrites in the Late Miocene vermetid carbonate bioconstructions, Salento Peninsula, Italy: Record of a microbial/metazoan association. *Sediment. Geol.* **2012**, *263–264*, 133–143. [CrossRef]
176. Guido, A.; Sposato, M.; Palladino, G.; Vescogni, A.; Miriello, D. Biomineralization of primary carbonate cements: A new biosignature in the fossil record from the Anisian of Southern Italy. *Lethaia* **2021**, *55*, 1–21. [CrossRef]
177. Guido, A.; Rosso, A.; Sanfilippo, R.; Miriello, D.; Belmonte, G. Skeletal vs. microbialite geobiological role in bioconstructions of confined marine environments. *Palaeogeogr. Palaeoclimatol. Palaeoecol.* **2022**, *593*, 110920. [CrossRef]
178. Guido, A.; Calcagnile, M.; Talà, A.; Tredici, S.M.; Belmonte, G.; Alifano, P. Microbial consortium involved in ferromanganese and francolite biomineralization in an anchialine environment (Zinzulùsa Cave, Castro, Italy). *Sci. Total Environ.* **2024**, *936*, 173423. [CrossRef]

179. Cipriani, M.; Apollaro, C.; Basso, D.; Bazzicalupo, P.; Bertolino, M.; Bracchi, V.A.; Bruno, F.; Costa, G.; Dominici, R.; Gallo, A.; et al. Origin and role of non-skeletal carbonate in coralligenous build-ups: New geobiological perspectives in biomineralization processes. *Biogeosciences* **2024**, *21*, 49–72. [CrossRef]
180. Kouwenhoven, T.J.; Seidenkrantz, M.S.; Van der Zwaan, G.J. Deep-water changes: The near-synchronous disappearance of a group of benthic foraminifera from the Late Miocene Mediterranean. *Palaeogeogr. Palaeoclimatol. Palaeoecol.* **1999**, *152*, 259–281. [CrossRef]